Korean J. Chem. Eng., 38(11), 2171-2194 (2021)
DOI: 10.1007/s11814-021-0926-x

pISSN: 0256-1115
eISSN: 1975-7220

INVITED REVIEW PAPER

Recent advances in three-dimensional bioprinted nanocellulose-based hydrogel scaffolds for biomedical applications

Anam Saddique and In Woo Cheong†

Department of Applied Chemistry, Kyungpook National University, 80 Daehak-ro, Buk-gu, Daegu 41566, Korea
(*Received 18 May 2021 • Revised 10 August 2021 • Accepted 12 August 2021*)

Abstract−Cellulose is the most abundant biopolymer on earth. Due to its excellent physical and biological traits, particularly its biocompatibility, biodegradability, and low cytotoxicity, it has become promising material for biomedical applications. Moreover, cellulose-based hydrogels are the best-suited for biomedical applications due to their biocompatibility and ability to be controllably molded into different shapes. Therefore, in recent years, a significant amount of research has been focused on preparing cellulose-based materials such as cellulose hydrogels with different morphologies and functional groups. Among the various methods used to prepare cellulose-based hydrogels, three-dimensional (3D) bioprinting has been used to generate these materials for drug delivery, tissue engineering, and scaffolds due to the customizability of their complex morphology. To date, many studies have been published on the important aspects of the bioprinting of cellulose-based hydrogels; however, despite an increasing amount of research in this area, various issues still exist that prevent their advanced applications. In addition, cellulose exists in various forms and, depending on its type, exhibits unique physical and rheological properties. It is, therefore, meaningful to fabricate advanced cellulose-based hydrogels only when the properties of the cellulose derivatives are well understood. In this review, the emerging approaches of the design and fabrication of advanced cellulose-based biomaterials (i.e., cellulose nanocrystals, cellulose nanofibrils, and bacterial nanocellulose) are discussed, as well as their roles in traditional and emerging (3D bioprinting) biomedical fields, mainly in drug delivery, wound dressings, tissue engineering, and scaffold applications.

Keywords: Nanocellulose, Hydrogel, 3D Bioprinting, Biomedical

INTRODUCTION

Cellulose is the most ubiquitous biopolymer on earth, with an estimated production of over 7.5×10^{10} tons per year. This natural polymer has extraordinary chemical and physical properties and is regarded as being a virtually limitless raw material, the use of which would greatly aid the ever-expanding requirements of green and biocompatible products. Over the past few years, cellulosic fibers have been used as a raw material to produce a wide range of products, including paper, textiles, and nutritive fibers. Wood is the leading source of cellulose used as a raw material in the pulp and paper industry. However, plants (including flax, hemp, jute, ramie, and cotton) are also a source of a massive quantity of this polysaccharide. Likewise, certain algae, bacteria, fungi, and several marine animals (e.g., tunicates) also generate cellulose [1-4]. The percentage of cellulose content varies according to its source of origin, as shown in Table 1.

Table 1. Percentage cellulose content in different plants

Source	Cellulose content (%)	References
Rice husk		
Aho (Autumn variety)	94.2	[5]
Boro (Summer variety)	89.5	[6]
Cotton fibers	85.0-90.0	[7]
Eucalyptus	76.0	[8]
Flax fiber	72.0	[9]
Rice straw	71.0	[10]
Hemp fibers	68.0	[7]
Sisal fibers	65.5	[11]
Corn silage	32.1	[12]
Archira	19.1	[11]
Banana	16.6	[10]

From a structural perspective, cellulose is a polysaccharide, a high molecular weight homopolymer composed of β-1,4-anhydro-d-glucopyranose units as depicted in Fig. 1. These units adopt a chair-like conformation for consecutive glucose molecules rotated by a 180° angle about the molecular axis with a hydroxyl (-OH) group in an equatorial position. Besides this, concerning its molecular axis, the cellulose chain has directional asymmetry with a hemiacetal group on one end and an -OH group on the other. Depending on its source, the degree of polymerization (DP) of cellulose chains varies with an estimated 10,000 glucopyranose units in wood cellulose and 15,000 in native cotton cellulose [13].

Cellulose has the distinctive attribute of containing three -OH groups per monomer. The potential for these -OH groups to form hydrogen bonds plays a vital part in the development of semi-crystalline and fibrillar packing, which dominates the physical attributes of these remarkably interconnected biomaterials. In nature,

†To whom correspondence should be addressed.
E-mail: inwoo@knu.ac.kr

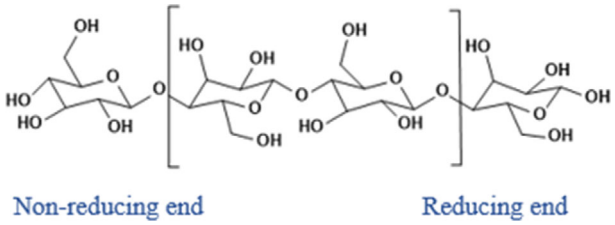

Fig. 1. Chemical structure of a cellulose molecule.

cellulose does not exist as discrete molecules, existing instead in the form of assemblies. At the site of its biosynthesis, individual cellulose molecules undergo spinning in an ordered direction to form these assemblies [14].

Based on the morphological features of cellulose, the transverse dissociation of fibers in its amorphous regions present beside its molecular axis leads to the formation of nanometer-scale and highly crystalline rod-like fragments, referred to henceforth as cellulose nanocrystals (CNCs). Cellulose nanofibrils (CNFs) can be synthesized via the lateral disintegration of cellulose fibers into substructural nanoscale units (nanofibrils) via mechanical shearing. Microorganisms can also produce this biomaterial with nanosized dimensions to generate a form of cellulose referred to as bacterial nanocellulose (BNC).

Due to their high surface area and consistent particle size distribution, cellulosic materials tend to exhibit mechanically stable self-assembled structures [15,16]. Recently, self-assembled CNCs [17] and CNF [18,19] hydrogels synthesized via a crosslinking approach have been revealed to be potential materials for use in biomedical applications due to their remarkable mechanical stability, well-regulated morphology, and excellent biocompatibility [20]. Alternatively, integrating CNCs or CNFs into a natural polymer (e.g., alginate, gelatin) or synthetic (e.g., polyacrylamide [PAM], poly(vinyl alcohol) [PVA] poly(ethylene glycol) [PEG]) matrices may lead to the formation of mechanically stable hydrogels, which have been widely investigated for use in biomedical applications [18,21]. Recently, numerous reviews have detailed the use of cellulose nanomaterial-containing hydrogels for different applications (e.g., tissue engineering, biomaterials, drug release, and wound repairing), to which the readers are directed for further reading [22-26].

Recently, three-dimensional (3D) printing, often referred to as bioprinting, has been gaining significant attention for use in hydrogel-based ink materials, to generate scaffolds for regenerative biomedical applications. However, despite this great interest, there are few comprehensive reviews on cellulose-based 3D bioprinting. Many elaborated reviews are still restricted to the traditional approaches of synthesizing CNC-, CNF-, and BNC-containing hydrogels. Hence, in the present review, the advanced fabrication of chemically modified cellulose is highlighted, detailing the replacement of one of its local hydroxyl groups with functional groups, such as specific acids, chlorides, and oxides. In this way, materials with desirable and promising 3D-bioprinting characteristics can be prepared for use in the biomedical field, mainly in drug delivery, wound dressing, and tissue engineering, as unmodified cellulose has several less suitable characteristics that hinder its direct use in biomedical applications, such as its low dispersibility in water and the most common solvents, moisture sensitivity, and low resistance against microbial assault.

Table 2. Summary of bioprinting types, highlighting their advantages, disadvantages, and other specific properties

	Extrusion bioprinting	Inkjet bioprinting	Laser-based bioprinting	Stereolithography
Advantages	Simple, with the capability of being able to print different biomaterials, with high cell density, as shown in **Fig. 3(a)**.	Capable of printing low-viscosity biomaterials, high-speed fabrication, cheap, with high-resolution, as shown in **Fig. 3(b)**.	Nozzle-free system, bioprinting time free from complications, superior accuracy, and cell viability, as shown in **Fig. 3(c)**.	High-resolution, accumulation of biomaterials in the liquid or solid-state, as shown in **Fig. 3(d)**.
Disadvantages	Only uses viscous liquid	Intrinsic incapability to deliver a constant flow, inadequate functionality for erect structures, short cell density.	Poor mechanical properties, long fabrication time, damages cells due to heat energy generated from the laser, creating aggregates in the final tissue scaffolds.	Requires support material, extensive and laborious post-processing, difficult to use to fabricate large scaffolds that have a complex internal structure.
Speed	Slow	Fast	Medium	Fast
Viscosity	30.6×10^{7} mPa s	<10 mPa s	1-300 mPa s	No limitations
Vertical bioprinting capability	Good	Poor	Medium	Good
Cell viability	89.46±2.51%	80%-90%	<85%	>90%
Cell density	High	Low	Medium	Medium
Resolution	100 μm	50 μm	10 μm	100 μm
Cost	Moderate	Low	High	Low

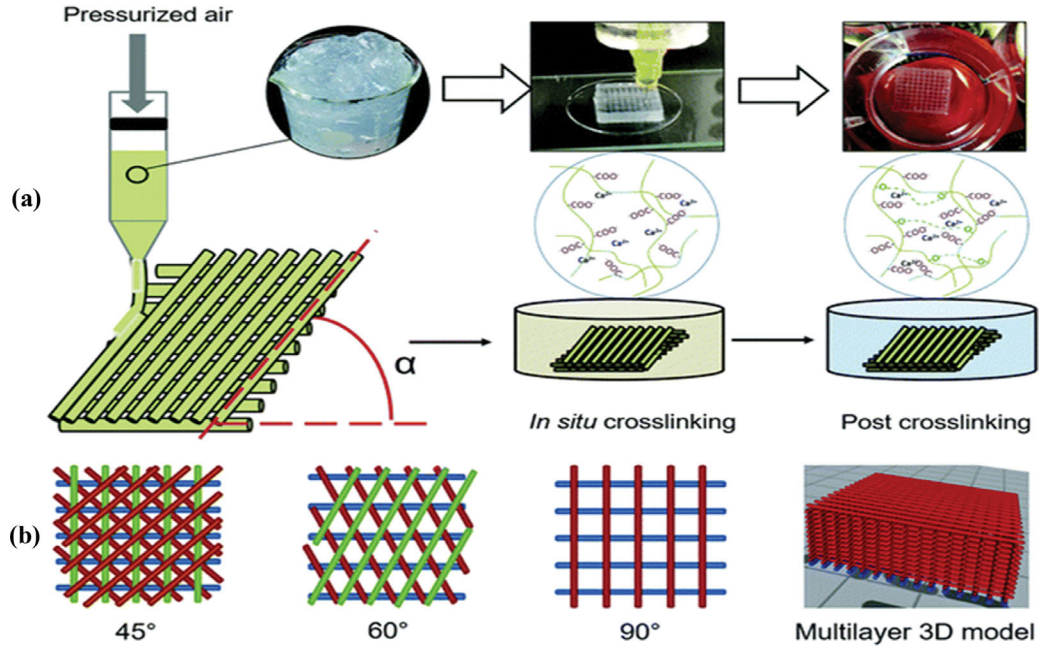

Fig. 2. Illustration of the three-dimensional (3D) bioprinting of cellulose nanofibril hydrogels: (a) graphical illustration of the bioprinting methodology and a dual step crosslinking approach and (b) bioprinting models; top views of 45°, 60°, and 90° patterns and a 3D view of the 90° scaffold model [37]. Adapted with copyright permission from the Royal Society of Chemistry.

THREE-DIMENSIONAL BIOPRINTING OF CELLULOSE-BASED HYDROGELS

Three-dimensional bioprinting is a rapid prototyping and additive manufacturing (AM) method. Since the early 2000s, it has been used in medicine to produce customized prostheses and dental implants [27,28]. The 3D structured materials are commonly generated using AM technologies such as direct ink writing, standard lithography, laser-based polymerization, or epitaxial assembly techniques [29].

Three-dimensional bioprinting technology is used in biomedicine to accumulate precise data on tissues and organs to aid the design of models, transfer respective data into an electrical signal to regulate the printing, and generate a printing process to control the cell feasibility during the process of fabrication. The types of 3D-bioprinting along with their specific advantages and disadvantages are elaborated in Table 2.

The application of 3D bioprinting in biomedical engineering can be divided into four categories: (i) the development of long lasting non-bioactive material implants, (ii) the fabrication of biodegradable and native bioactive scaffolds, (iii) the development of a model of a compulsive organ to assist pre-operative development and analysis of surgical treatment, and (iv) the direct 3D bioprinting of tissues and organs that have entire life functionality [30]. Most recently, the term "3D bioprinting" has been employed progressively to signify the 3D bioprinting of structures using biocompatible inks (generally labeled as bio-inks), which contain living cells, fabricated biomaterials, and vital nutrients [31,32]. The 3D bioprinting of hydrogels usually involves three steps: (i) the design and development of templates, (ii) printing using bio-inks, and (iii) in situ and/or a post-bioprinting crosslinking method for stabilizing the printed structures [33-36]. Fig. 2 shows a graphical illustration of the 3D bioprinting of nanocellulose-containing hydrogels. The capability of bioprinting with ink via a micro nozzle is the key aspect in this process as it allows the control of the quality of the fabricated structures, as illustrated by the rheological attributes of the ink that help it to flow and retain its printed shape, inhibiting the deformation of a single filament [34]. Furthermore, biocompatible inks capable of forming cross-links over a short distance at body temperature, in the presence of a low concentration of photoinitiator, or requiring low-intensity ultraviolet (UV) light are promising materials for use in 3D bioprinting [37].

TYPES OF NANOCELLULOSE

Two major types of nanocellulose can be isolated from lignocellulose biomass, e.g., CNFs and CNCs, alongside nanocellulose obtained from bacteria that are referred to as bacterial nanocellulose [39-41]. The nanocellulose type is important, as the different types show different characteristics in terms of enzymatic hydrolysis, cell adhesion and growth, surface functionalization, degree of substitution, and their consequent physicochemical properties. In this section, the preparation and characteristics of nanocellulose are introduced, which are receiving a great amount of attention in the pursuit of nanocellulose hydrogels.

1. Preparation and Characteristics of Cellulose Nanocrystals

CNCs are generally crystalline materials, referred to as cellulose nano whiskers (CNWs) or nanocrystalline cellulose (NCC), which have firm rod-like structures that are 10-30 nm in diameter and have lengths of >100 nm. The conventional way of synthesizing CNCs is via the hydrolysis of cellulose using strong inorganic acid, such as hydrochloric [42,43], sulfuric [44], phosphoric [45], hydro-

bromic [46], or nitric [47] acid. The most frequently used is sulfuric acid, which is used to prepare sulfonated CNCs that exhibit excellent dispersibility in water [48,49]. During hydrolysis using sulfuric acid, the amorphous regions of the cellulose are degraded, while the crystalline regions remain intact as a result of their intrinsic structural stability [40,50]. The insertion of sulfate half-ester factions on the backbone endows the CNCs with excellent dispersibility in water [51]. Overall, acid hydrolysis is an easy and rapid approach for the preparation of CNCs [52]. However, there are still several issues with this method that need to be addressed, such as the requirement of a large volume of water, severe corrosion of the apparatus, severe environmental contamination, and a comparatively low product yield compared to other methods. Thus, recently, more viable approaches based on the use of biodegradable reagents have been designed to tackle the issues mentioned above, for example, the use of solid acid hydrolysis (e.g., phosphor tungstic acid) [53], organic acid hydrolysis (e.g., formic acid, oxalic acid) [54], and treatment with ionic liquids [55] or deep eutectic solvents [56]. The rod-like structure of CNCs endows them with a unique combination of characteristics, such as high axial stiffness (~150 GPa), high tensile strength (estimated at 7.5 GPa), low coefficient of thermal expansion (~1 ppm/K), the thermal stability of up to ~300 °C, a high aspect ratio (10-100), low density (~1.6 g/cm^3), and shear-thinning rheology when in suspension. The exposed -OH groups on the surface of CNCs can be readily modified to achieve different surface properties, with this technique being used to adjust the self-assembly and dispersion of CNCs for a wide range of suspensions and matrix polymers and to control the interfacial properties of composites [42-44].

2. Preparation and Characteristics of Cellulose Nanofibers

CNFs, also referred to as nano-fibrillated cellulose, are 5-60 nm in diameter with a flexible fiber-like morphology, made up of both crystalline and amorphous domains. These materials can be primarily synthesized via the mechanical treatment of cellulosic fibers, using ultrasonication, high-pressure homogenization, grinding, and micro fluidization [57,58]. Among these techniques, high-pressure homogenization is most widely used to develop CNFs that exhibit excellent properties [59]. Pressurized homogenization can generate distinct types of forces, such as high-rate pressure, high-rate speed, high turbulence, and shear via fast variation in the pressure, causing a rupture in the CNFs, ultimately releasing accumulated nanofibrils [60]. The preparation of CNFs via a mechanical fibrillation approach requires intensive energy. Several pretreatment approaches have been developed to decrease the expenditure of energy that is required in the mechanical deconstruction of CNFs in this way, techniques such as hydrolysis using enzymes [61], (2,2,6,6-tetramethylpiperidin-1-yl) oxyl (TEMPO)-mediated oxidation [62,63], carboxymethylation [64,65], and quaternization [66]. After pretreatment, the number of charges on the backbone of fibrillar cellulose decreases, meaning that the input of power is required in the fibrillation approach in order to improve the colloidal strength of the resulting CNFs [58]. For instance, when oxidizing using TEMPO, a huge number of carboxyl groups are created on the backbone of the cellulose, which leads to the selective oxidation of the cellulose C6 hydroxyl group to a carboxylate group. After moderate mechanical degeneration, a clear gel-like CNF suspension might be achieved. Moreover, after oxidation with TEMPO, the utilization energy of the material is around 570 KWh/t, which is considerably lower than that of the 70,000 KWh/t exhibited by the material with no pretreatment [67-69]. Another approach can be used to create positive quaternary trimethylammonium groups on the backbone of fibrillar cellulose to enhance its static repulsion [70] and ultimately improve the nano fibrillation of this material [66]. Other approaches that use this cationic pretreatment method have been developed, which have shown a five-fold decrease in the utilization of energy at the fibrillated phase. Remarkably, the created cationic groups endow the resultant CNFs with antibacterial activity, making them useful for wound repairing, tissue engineering, and food packaging applications. The CNFs exhibit excellent mechanical properties, such as a high aspect ratio (4-20 nm), an intrinsic strength of 1-3 GPa, a low density of ≈1.5 g/cm^3, and a crystal modulus of 138 GPa.

3. Preparation and Characteristics of Bacterial Nanocellulose

BNC is a nanofibrillar extracellular polysaccharide generated by different types of bacteria [71]. These bacteria generate BNC in different media using various sources of carbon, with the efficiency of the production of BNC significantly dependent on the growth substrate used in their generation. The substrate provides momentum to promote the bacterial metabolic rate throughout the consumption of extensive energy, which is the pathway to producing cellulose. Ideally, the bacterial cells should be able to convert carbon into glucose to be used in the synthesis of cellulose [72].

Among bacteria, the capability of producing BNC is common. *Komagataeibacter (K.) xylinus* is the most well-known species of bacteria that produce BNC, with this capability relating them to the acetic acid group of bacteria. These bacteria are rigorously aerobic gram-negative bacteria that can be categorized as proteobacteria [73,74]. This type of species was recognized as *Acetobacter xylinum* for many years but later grouped into *Gluconacetobacter xylinus*. After this, owing to additional taxonomical alterations, it was reclassified as *K. xylinus*. Among the acetic acid-containing bacteria, *K. xylinus* is not only the only species that has great capability of producing BNC; other species such as *K. medellinensis*, *K. hansenii*, *K. nataicola*, *K. rhaeticus*, *K. oboediens*, *K. pomaceti*, and *K. saccharivorans* are also robust producers of cellulose [75,76]. A crucial characteristic of utilizing acetic acid-containing bacteria in the synthesis of cellulose is that the end product is of food-grade quality.

BNC is produced in bacterial membranes from nucleotide-stimulated glucose. Bacteria feed BNC through holes in the cell membrane to form fibrils composed of D-glucose components, which have 1,4-glycosidic bonds. The fibril sequences are linear and squeeze out from the cell. So, the adjacent and affiliated sequences form inter- and intra-chain hydrogen bonds between all available hydroxyl groups. In this way, the chains blend into insoluble nanofibrils 1-9 nm in length and 25 nm in width, equivalent to 2,000-18,000 glucose residues [77]. These types of nanofibrils further accumulate into <100 nm-wide ribbon-like fibrils that endow the BNCs with strong advantages, such as hydrophilicity, moldability, and crystallinity. While nearly all the -OH groups of the cellulose polymer are involved in hydrogen bonding, each region of cellulose contains an inherent C4-hydroxyl group and the inverse region

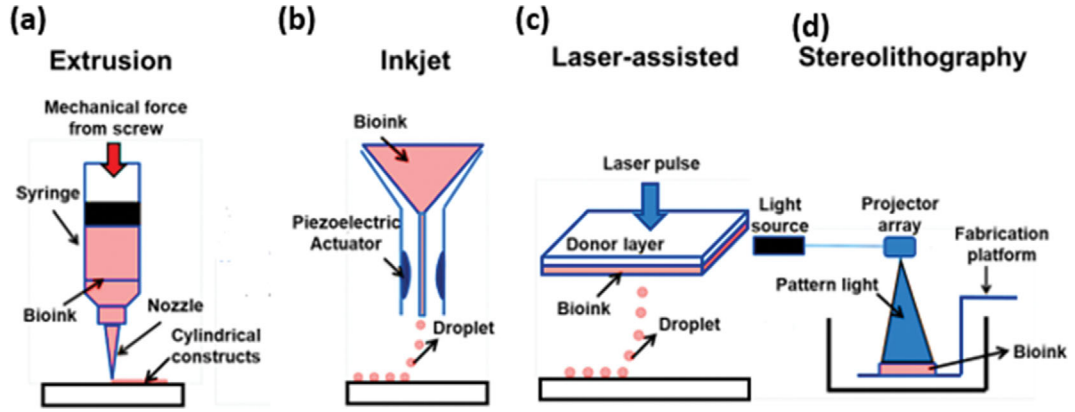

Fig. 3. Schematic diagram showing the types of three-dimensional (3D) bioprinting. (a) In the extrusion technique, mechanical force is required for the deposition of ink; (b) the inkjet method requires the use of a piezoelectric actuator to deposit ink; (c) in the laser-assisted system, the laser excites an energy-absorbing donor layer coated with the ink, which causes fizzing at the border of the ink layer and results in its deposition in the form of droplets; and (d) stereolithography exposure of a light-curable resin requires a precise source of light to pattern a binary image to create a 3D structure [38]. Adapted with the permission of a creative commons license. Copyright 2019, Published by Hapres Co., Ltd.

contains a free C1-hydroxyl group, with both regions representing potential sites for the chemical modification of cellulose [78,79].

As BNC is free from lignin, hemicelluloses, and pectin, there is no need to purify it using harsh chemical processes, such as acid hydrolysis and alkaline treatment. Instead, BNC can be readily purified via a low-energy process. In comparison to plant cellulose, BNC exhibits high crystallinity (70%-80%), purity, high-water holding capacity (99%), a high DP (up to 8000), good mechanical strength (>2 GPa), a unique nanostructure, and is non-toxic, while also retaining its biocompatibility. Typically, a ribbon of bacterial nanofibril has a width of around 60 nm and an indefinite length, while softwood pulp fibers are normally at least 100 μm wide. Due to this thickness of its fibrils, BNC has a surface area that is around 200 times higher than that of softwood pulp fibers. This high surface area and hydrogen bonding capability mean that BNC can retain up to 700% of its weight in water [80].

SYNTHESIS OF NANOCELLULOSE-BASED HYDROGELS VIA THREE-DIMENSIONAL BIOPRINTING

Hydrogels were first proposed and designed in the 1960s by Wichterle and Lím [81]. From that point onwards, hydrogels gained enormous attention, both in academia and industry. Nowadays, hydrogels are used in a broad range of applications, such as soil conditioners, food additives, hygiene products, and biomedical applications [82]. Hydrogels are a heterogeneous mixture of two or more phases, which generally comprise a solid 3D network as a solid phase and water as the dispersed phase [83]. The synthesis of hydrogels that have high moduli is challenging and is the key limitation in practical applications [84]. Some applications require the use of a material that needs to be able to sustain its shape over a long period or be deformed without sustaining any fractures. For example, materials that are used in place of articular cartilage require properties of high toughness and high stiffness (Young's modulus of 1 MPa). However, traditional hydrogels exhibit low values such as <10 kPa, <100 kPa, and <100 J/m^2 for stiffness, tensile strength, and toughness, respectively [85,86].

Due to their mechanical properties, CNCs, CNFs, and BNC are extensively used as fillers in polymer composites [87,88]. However, the hydrophilic environment of cellulose or the insertion of hydrophilic groups during its pretreatment has made it challenging to effectively disperse nanocellulose in common polymers (e.g., polylactic acid [PLA], polyethylene [PE], and polypropylene [PP]). Although some modification approaches, e.g., esterification [89], silylation [90], and polymer grafting [91], have been explored to tackle this problem, such techniques are typically slow and require the use of harmful reagents, which hinders their industrial application [92]. However, hydrophilic CNCs, CNFs, and BNC with a charged interface are extremely useful as fillers or even as building blocks of hydrogels. So far, there has been an extensive amount of research carried out on the synthesis of CNC-, CNF-, and BNC-containing hydrogels via physical or chemical approaches, which show efficient improvement in the resultant nanofillers or interaction with the matrices of polymers. The various reported approaches of incorporating CNCs, CNFs, and BNCs into a polymer matrix or direct synthesis of the self-assembled hydrogel are summarized in Table 3 alongside their specific applications in the biomedical field.

1. Cellulose Nanocrystals-based Hydrogels

Usually, due to their rigid structure and low aspect ratio, CNCs are incapable of self-forming a mechanically stable hydrogel. However, modifying the surface chemistry of CNCs or generating a crosslinking network leads to the formation of mechanically stable hydrogels [17,117]. CNCs are highly appropriate materials for use as filler agents due to their excellent dispersibility, crystallinity, and they can be mixed into the polymeric network of a hydrogel via chemical or physical approaches [1]. Until now, several kinds of approaches such as simple homogenization [118,119] cyclic freeze-thaw methods [120,121], free radical polymerization [122,123], UV/ion facilitated crosslinking [124,125], and 3D bioprinting [126,127] have been used to integrate CNCs with different types of polymer networks, such as PVA, PEG, and PAM, as well as sev-

Table 3. Summary of different approaches used to synthesize cellulose nanocrystals, cellulose nanofibrils, and bacterial cellulose-based hydrogels and their developed biomedical applications

Material	Surface chemistry	CNC wt% (vs. polymer)	CNC total wt% (in gel)	Hydrogel synthesis method	Storage modulus	Compressive modulus	Intended application	References
PVA, CNC	Sulfate half-ester	0-7	0-0.7	Freeze-thaw		800-1,100	Wound dressing	[93]
PVA, borax, CNC	Sulfate half-ester		1	Homogenization	0.12-0.65	0.9-4.8	Wound dressing	[94]
PSA, CNC	Sulfate half-ester	1.25-24.3		Free radical polymerization			Wound dressing	[95]
PNIPAM, clay, NC	Sulfate half-ester	0-8	0-0.8	Freezing, free radical polymerization	6-15		Drug delivery	[96]
Cyclodextrin-g-CNC	Polymer-grafted	0-5.96		Homogenization			Drug delivery	[97]
CNC, chitosan-g-PAA	HCl hydrolyzed	0-10		Free radical polymerization			Drug delivery	[98]
CNC-gelatin	Sulfate half-ester	0-25		Homogenization, casting, drying			Drug delivery	[99]
Alginate, CNC	Cationic (HPTCMAC)	10	0.10	Ionic crosslinking			Drug delivery	[100]
Alginate, gelatin, CNC	Sulfate half-ester	0-2	0-0.04	Ionic crosslinking, injectable		50-92	Tissue engineering	[101]
Cellulose, CNC	Cationic (HPTCMAC)	0-50	0-3.5	Homogenization			Drug delivery	[102] Continued
PVA, CNC-g-AA-C-AMPS	Polymer-grafted	50-90	0.5	Free radical polymerization			Drug delivery	[103]
GMA, PVA, CNW, starch	HCl hydrolyzed	0-10	0-5	Homogenization, emulsion polymerization			Drug delivery	[104]
HA, CNC	Aldehyde	0-33	0-0.5	Coextrusion (injectable)	107-152		Tissue engineering	[105]
Collagen, gelatin, microspheres, CNC	Sulfate half-ester	0-10		Homogenization, freeze-drying			Angiogenic tissue engineering	[106]
CNFs	Carboxymethylated	100	0.14	Homogenization, pH reduction	0.1-1		Cell templating	[107]
CNFs	Unspecified	100	1	Homogenization (injectable)			Radiolabeling for drug release	[108]
CNFs	COOH	100		Homogenization, salt bridging			Tissue culture	[109]

eral varieties of natural polymers, including gelatin and alginate. For instance, the use of a freeze-thaw method has been reported in the preparation of CNC/PVA hydrogel composites [121]. In this study, we observed that the CNCs play a vital role as nucleation sites that promote the synthesis of the composite hydrogels which exhibit enhanced barrier and mechanical attributes. In another study, the impact that the aspect ratio and surface charge of CNCs have on the strengthening of the properties of CNC/PAM nanocomposite hydrogels were explored [128]. The findings of this study showed that a higher number of surface charges of the materials

Table 3. Continued

Material	Surface chemistry	CNC wt% (vs. polymer)	CNC total wt% (in gel)	Hydrogel synthesis method	Storage modulus	Compressive modulus	Intended application	References
CNFs	COOH	100	1	Sacrificial templating, centrifugation			Tissue engineering	[110]
CNFs, PVA, borax	COOH	20-60		Homogenization		28-97	Wound dressing	[111]
NVP, CNFs	Carboxymethylated		0-1.6	Photopolymerization			Nucleus pulposus implant	[112] Continued
CNFs, gelatin, chitosan	Unspecified	70-90		Homogenization		1,000-3,000	Articular cartilage implant	[113]
CNFs, hemicellulose	Aldehyde, COOH	70-100	0.10	Homogenization			Wound healing	[114]
BNC, alginate	Unspecified			Solution impregnation			Wound healing	[115]
BNC, AM	COOH			Microwave irradiation			Wound healing	[116]

led to their better dispersibility and acted as a useful way of transferring stress in the materials. Moreover, the mechanical strength of the materials was enhanced via the use of CNCs with a high aspect ratio.

Recently, owing to its accuracy, speed, and flexibility, 3D bioprinting has been examined as a favorable and efficient procedure to synthesize CNC-containing hydrogels [126]. As shown in Fig. 4(a), a hydrogel nanocomposite scaffold of CNC, gelatin, and sodium alginate (SA) was manufactured via 3D bioprinting. First, the CNCs, gelatin, and SA were blended to develop a hydrogel with the composition 70/20/10 (wt%). In this way, a 3D hydrogel framework was printed that exhibits a distinct structure. Finally, dual crosslinked hydrogel scaffolds were achieved via the crosslinking of the hydrogel using glutaraldehyde and calcium chloride ($CaCl_2$) [129].

Also, 3D-printed CNC-loaded poly (ethylene glycol) diacrylate (PEGDA) hydrogels have been prepared using stereolithography (SL), as shown in Fig. 4(b). In the preparation of these hydrogels, the PEGDA-CNC precursor was initially synthesized via photoinitiated free radical polymerization at room temperature. Subsequently, PEGDA-containing CNC-loaded hydrogels with various structural designs were printed using an SL system via in situ photopolymerization. Hence, it was found that the integration of CNCs might enhance the physiochemical and thermomechanical activity of the resultant printed nanocomposites, subsequently improving the surface wettability and toughness of the PEGDA-CNC hydrogels. For the first time, this research showed an effective presentation of the 3D-bioprinting of CNC nanocomposite hydrogels using SL, developing a dense structural design with improved properties, with the resultant 3D-printed nanocomposite hydrogels being potentially suitable for use in tissue cultures and reconstructive surgical treatment due to the biocompatibility of their precursor. This analysis suggests that the resultant nanocomposite hydrogels are suitable for use in industrial applications, as well as assisting further research in this area [126].

Due to its aforementioned benefits, SL 3D bioprinting is a novel manufacturing system and can be used to perform several crucial functions in different disciplines, such as in medical engineering, in which patient-specialized materials are essential. The use of this method presents advantages such as the novel growth of materials, failure scrutiny of new material functionalities, uniform production of highly tailored products, and the profitable delivery of innovative materials. Therefore, 3D bioprinting is rapidly becoming a useful fabrication system, the use of which will be of utmost importance medical engineering.

Recently, multicomponent cell-free hydrogel inks, consisting of SA, carboxylate CNCs (cCNCs), and xyloglucan (XG), were synthesized and examined in terms of their post-printing reliability in 3D-bioprinting for tissue engineering applications. Both cCNCs and XG provide the hydrogel inks with properties such as shear thinning, as well as a wide range of sites for crosslinking (-COO- and -OH groups) in the synthesis of 3D bioprinting-based hydrogel networks that exhibit improved printability. The cCNCs provide the BPCX hydrogel inks with nanoscale mechanical strength and dynamic toughness for better proliferation, cell adherence, migration, and differentiation, as shown in Fig. 4(c) and (d) [130].

2. Cellulose Nanofibrils-based Hydrogels

Like CNCs, semi-crystalline structured CNFs with a high aspect ratio display a significant propensity to form interwoven networks, which aids in the development of more mechanically stable hydro-

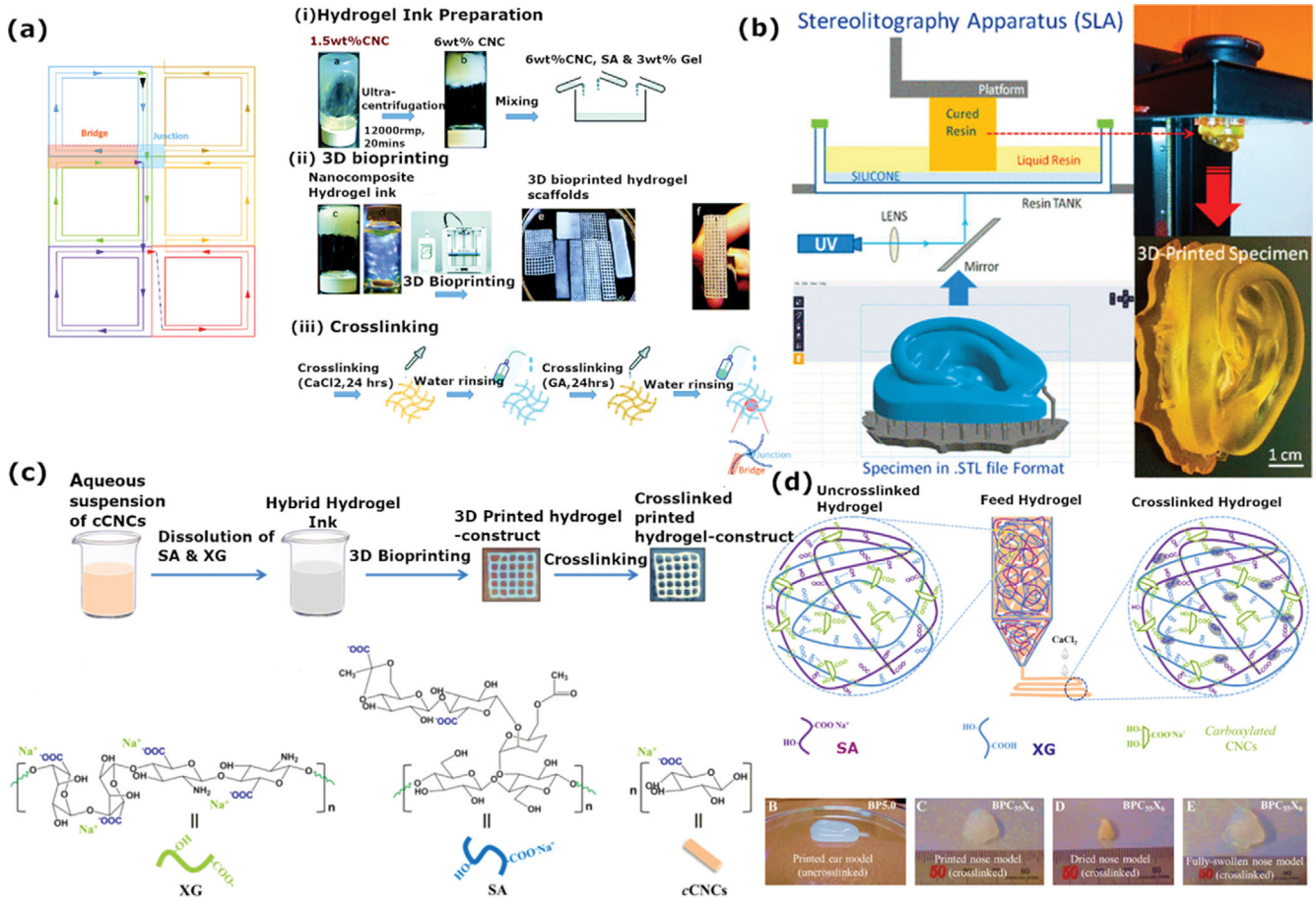

Fig. 4. Schematic diagram of the synthesis of cellulose nanocrystals (CNC)-based hydrogels; (a) graphical representation of the treatment route used to three-dimensional (3D) print CNC/sodium alginate/gelatin hydrogel scaffolds [128], adapted with copyright permission from the Royal Society of Chemistry; (b) schematic representation of a system used for the 3D bioprinting of poly(ethylene glycol) diacrylate-CNC hydrogels [126], adapted with copyright permission from the American Chemical Society; (c) schematic diagrams of the bioprinting of BPCX hydrogel ink; and (d) the crosslinking approach [130], reproduced from an open-access article, published by IOP Science.

gels [85]. Hydrogelated carboxylate CNFs, oxidized using TEMPO, have been synthesized using various metal cations, such as Ca^{2+}, Zn^{2+}, Cu^{2+}, Al^{3+}, and Fe^{3+} [131]. It has been shown that the storage moduli of these fabricated hydrogels are strongly interrelated with the valency of the metal cations and their binding strength with the carboxylate groups of the CNFs. The driving force behind the crosslinking was intended to form a screening impact on the surfaces of the CNFs, via the formation of strong metal–carboxylate bonds. Later, Fe^{3+}- and Ca^{2+}-based CNF-crosslinked hydrogels were reported as tissue culture substrates. It was discovered that Ca^{2+}-crosslinked hydrogels, when covalently bound to protein, exhibit excellent cellular connections and distribution, making them highly appropriate for use in biomedical applications [132].

Like CNCs, CNFs can also be used as reinforcing agents to synthesize hydrogel composites that exhibit promising mechanical properties, although the loading of CNFs is comparatively lower than that of CNCs owing to the tendency of the CNFs to become entangled. Furthermore, due to their semi-crystalline structure and high aspect ratio, more malleable hydrogels can be achieved via their integration with CNFs. A CNF-PAM-reinforced hydrogel composite has also been reported. It was observed that the loading of a small amount of CNFs (0.0125-1 wt%) into the hydrogel significantly enhanced its extensibility, toughness, and strength of its dual network [133]. In an alternative example, a malleable, very strong, and anisotropic hydrogel-containing CNFs and PAM was developed for the treatment of muscle tissue. The resultant hydrogel has an anisotropic arrangement comparable to that of muscles and can be reversibly distorted without any prominent structural variations. It was discovered that resultant hydrogel has a tensile strength of 36 MPa on its longitudinal side due to the strong bonding and crosslinking of the CNFs and PAM polymer [134].

Three-dimensional bioprinting is a promising method that has been used to produce CNF-containing hydrogels. An example of this is in the dual-step fabrication of bioactive gyroid scaffolds created via the sacrificial templating of chitin nanofibrils (ChNFs) and CNF hydrogels. As demonstrated in Fig. 5(a), the gyroid template was first synthesized using micromirror layered lithography. Subsequently, hydrogels of CNFs and ChNFs were loaded into the template via centrifugation. Finally, the sacrificial template was dispersed in an alkaline solution to generate the gyroidal hydrogels

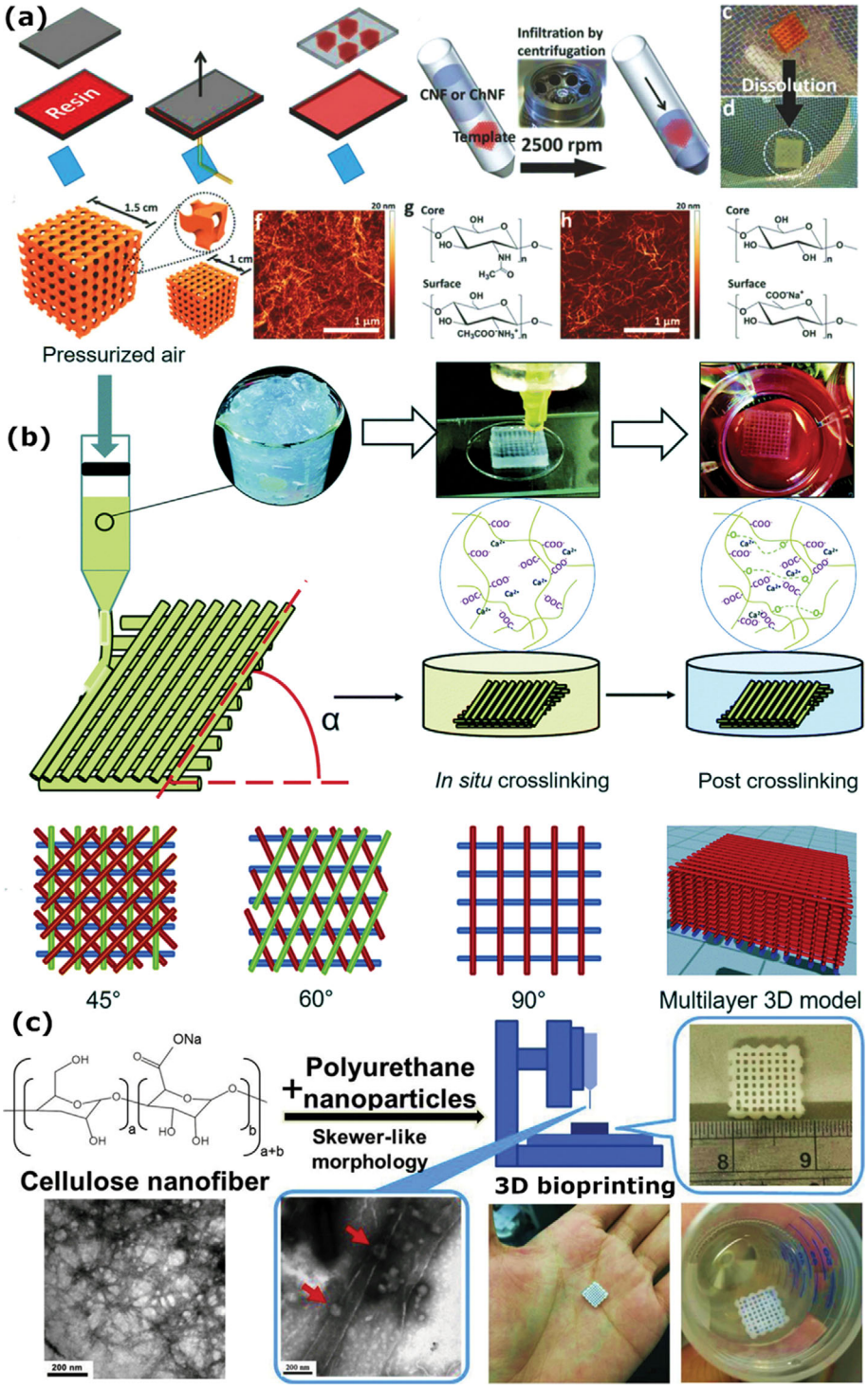

Fig. 5. Overview of the three-dimensional (3D) bioprinting of cellulose nanofibril-based hydrogels; (a) preparation of gyroid sacrificial templates via layered micromirror lithography [135], reproduced with permission from John Wiley & Sons; (b) graphical representation of the bioprinting methodology and the two-step crosslinking strategy showing 45°, 60°, and 90° bioprinted patterns and a 3D view of the 90° scaffold model [37], adapted with copyright permission from the Royal Society of Chemistry; and (c) schematic illustration of the 3D bioprinting of cellulose nanofiber-based polyurethane composites [137], reproduced with copyright permission from Elsevier.

[135]. An alternative method was used to design composite hydrogels containing gelatin methacrylamide (GelMA) and CNFs via a 3D bioprinting process. In this alternative preparation, the CNFs exhibited excellent shear-thinning properties and improved the mechanical strength of the resultant hydrogels [136].

Furthermore, as shown in Fig. 5(b), an effective method was developed to prepare 1 wt% TEMPO-oxidized nanocellulose hydrogel framework using a 3D bioprinting system. The 3D-bioprinted

scaffolds maintained their structural integrity via in situ crosslinking using Ca^{2+} cations, and their strength was further improved by post-printing covalent BDDE crosslinking. In this way, the mechanical properties of the scaffolds can be well adjusted on a 3-8 kPa scale. Cell viability tests proved that 1 wt% of the resultant scaffolds are not harmful to fibroblast cells [37].

A novel, directly printable, and high viscosity CNF-containing polyurethane (PU) composite ink was developed in another study. As shown in Fig. 5(c), the insertion of CNFs in situ during the production of waterborne PU and the direct addition of extra neutralizer triethylamine (TEA) following the CNFs (to attenuate the negative electron repulsion) efficiently enhanced the viscosity of the composite. The resultant ink shows excellent shear-thinning properties and is directly printable via 3D bioprinting for use in tissue engineering [137].

3. Bacterial Cellulose-based Hydrogels

BNC frameworks are potential candidates for use in biomedical applications as they have a biocompatible 3D composition, high purity, high porosity, and a high surface area [138-140]. Although, these BNC frameworks have some shortcomings, such as a lack of antibacterial properties and poor mechanical strength, which limit the scope of these materials for use in biomedical applications such as wound dressing and bone tissue cultures, respectively. To improve the mechanical and biological properties of BNC composites, different nanoparticles and polymers have been incorporated into these materials. In its natural state, BNC has a hydrogel structure and can be used as a matrix in the design of composites. In contrast, BNC nanocrystals (BCNCs) and BNC nanofibrils (BCNFs), generated from BNC using various methods, can be readily incorporated into polymer networks as reinforcing agents.

Numerous nanomaterials, such as ZnO, Ag, and TiO_2, have been introduced into BNC materials to produce composite scaffolds that have tremendous antibacterial properties [141]. In one case study, BNC/ZnO antibacterial composite hydrogel frameworks were prepared using a solution plasma process. BNC hydrogels with a 3D porous configuration show good coordination toward ZnO and act as excellent support materials. The obtained BNC/ZnO composites exhibit good antibacterial activity against *Staphylococcus aureus* and *Escherichia coli*. Another approach was developed to synthesize BNC-containing titanium dioxide (TiO_2) nanocomposite hydrogels via a facile sol-gel in situ impregnation method. The BNC/TiO_2 nanocomposite hydrogels exhibit great prospects for use in photocatalytic and antibacterial applications.

Along with antibacterial properties, BNC scaffolds have been endowed with mechanical and electrical properties via their integration with materials such as graphene (G) and carbon nanotubes to prepare BNC/nanomaterial composites. Among the reinforcing nanofillers used in the synthesis of polymer composites, G shows great potential as a nanofiller. However, the uniform dispersion of G in a polymer matrix is challenging in the synthesis of nanocomposites [142-146]. To address this limitation, a layer-by-layer (LbL) approach has been developed to prepare homogeneous, ultra-strong G/BNC nanocomposite hydrogels, as shown in Fig. 6(a). The enhanced mechanical properties of the G/BNC nanocomposite hydrogels can be attributed to the binding of G nanosheets with BNC nanofibers. In a comparison of this material with pristine BNC hydrogels, the modulus and tensile strength of the nanocomposite hydrogels with a G content of 0.30 wt% were improved by 279% and 91% respectively [147].

Various polymers, both natural and synthetic (e.g., chitosan (CS), gelatin, alginate, PVA, PAA, and PAAm), have been used to enhance the antibacterial and mechanical properties of BNC scaffolds in the preparation of BNC/polymer composite hydrogels.

Among natural polymers, CS is a type of polysaccharide that exhibits antimicrobial properties and shows a good affinity to attach to BCNFs via physical interactions [148-153]. BCNF/CS-containing semi-interpenetrating network (semi-IPN) hydrogel scaffolds have been synthesized by blending a solution of CS with a suspension of BCNFs, followed by crosslinking with glutaraldehyde. The resultant hydrogels exhibit remarkably high thermal stability, mechanical strength, and tremendous antibacterial properties, as shown in Fig. 6(b) [154].

A methylene diphenyl diisocyanate (MDI) modified BNC/poly (N-isopropyl acrylamide) (BNC/PNIPAAm) composite hydrogel framework was synthesized via an in situ polymerization approach, as shown in Fig. 6(c). The results indicate that the BNC/PNIPAAm hydrogel composite exhibits anisotropic heat sensitivity. Moreover, the compressive strength of the composite is 40-times greater than that of the pristine PNIPAAm hydrogel. Therefore, the resultant composite hydrogel holds great potential for use in the biomedical field in artificial muscle implants [155].

As illustrated in Fig. 6(d), BCNFs/PAAm cluster hydrogels were synthesized by in situ polymerization using acrylamide monomers in a suspension of BCNF clusters. In these composite hydrogels, the BCNFs act as both a reinforcing and crosslinking agent. The hydrogen bonds that form between the BCNF clusters and PAAm chains improve the mechanical attributes of the resultant composite hydrogels, such as their toughness and ultra-high tensile strength, enormously improved stretchability, and superb shape reform ability. The BCNF/PAAm composite hydrogels exhibit a prominent strain of almost 99%, are devoid of fracturing, and instantaneously reestablish their original form after the removal of compressive force. Thus, these BCNFs/PAAm hydrogel scaffolds widen the scope of biomaterials in the biomedical field, as they can be used in the repair of bone and cartilage [156]. Although the mechanical properties of hydrogels can be improved via the use of a cross-linker, most crosslinkers, such as aldehydes, are toxic to the human body. Aldehydes are electrophiles and can thus form covalent bonds at the nucleophilic positions of biological targets [157]. It has been demonstrated that such type of bonding disturbs the function of biomolecules, leading to cytotoxicity [158]. Thus, in the pursuit of obtaining bio-friendly hydrogels, the use of toxic crosslinkers should be avoided. Therefore, the latest research has focused on alternative crosslinking strategies that are safe and economical, such as electron beam and gamma ray-based polymer radiation crosslinking approaches.

For instance, cobalt-60 gamma-ray irradiation methodology has been used to synthesize a BNC/AAm composite hydrogel, which shows considerably improved hydrogel swelling and melting point in line with an increase in the radiation dose [159]. Another example is the synthesis of BNC-containing PAA-based composite hydrogels via an electron beam irradiation approach. The irradiation dos-

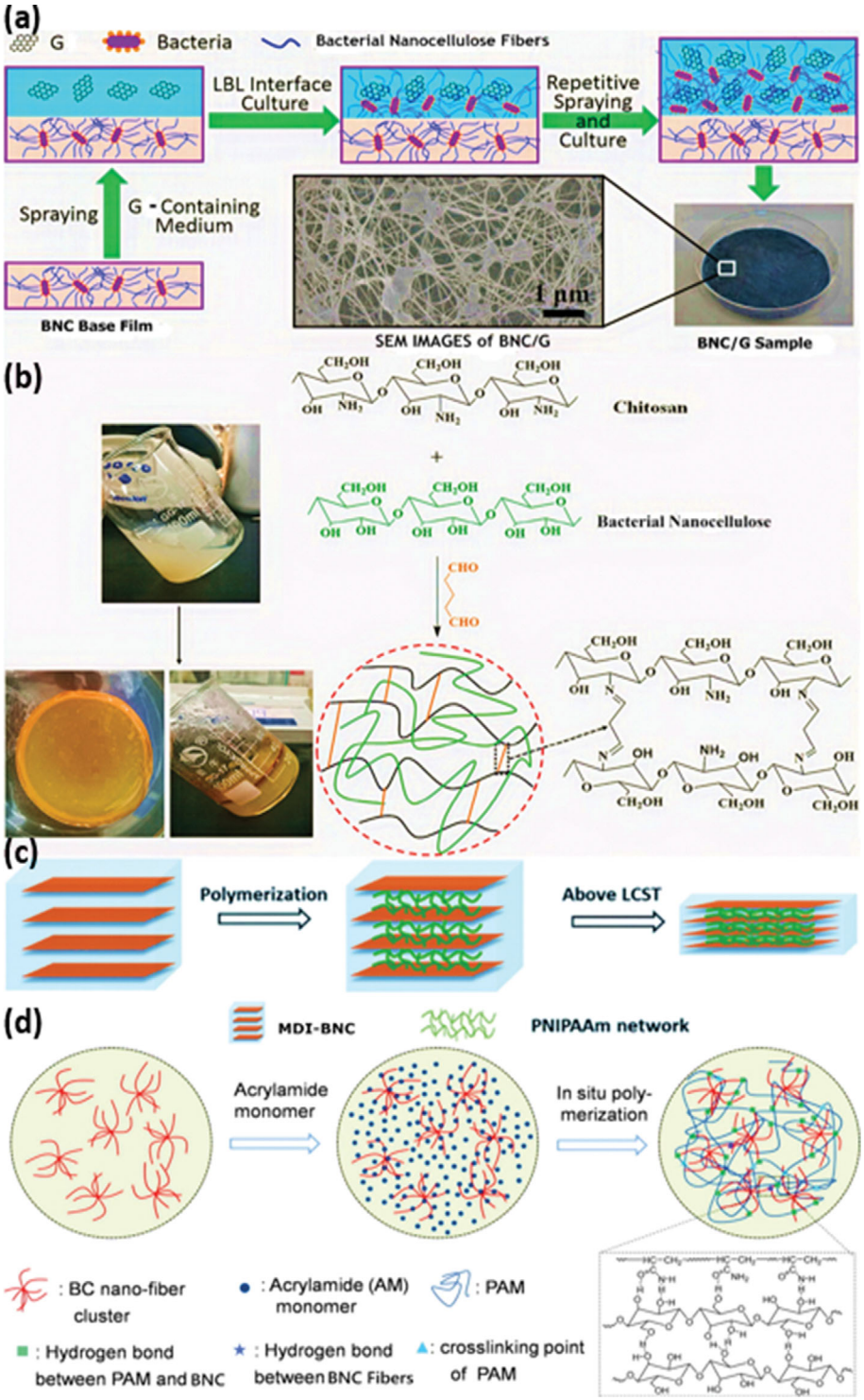

Fig. 6. Overview of the synthesis of bacterial cellulose (BNC)-based hydrogels: (a) schematic illustration of the preparation of a graphene/BNC nanocomposite via a layer-by-layer interface culturing approach [147], reproduced with copyright permission from Elsevier; (b) schematic representation of the formation of a BNC-chitosan hydrogel [154], reproduced with copyright permission from Elsevier; (c) schematic illustration of the formation of a methylene diphenyl diisocyanate-BNC/poly (N-isopropyl acrylamide) complex and its uniaxial deswelling above the LCST [155], adapted with copyright permission from the Royal Society of Chemistry; and (d) schematic representation of the preparation of a PAM/BNC hybrid hydrogel [156], reproduced with copyright permission from Elsevier.

age and AA concentration were found to have a significant effect on the physiochemical characteristics of the resultant composite hydrogels. A 60 : 40 ratio of BNC to AA and a 35 kGy dosage of electron beam radiations were shown to be the optimal properties

for preparing these hydrogels, which have decent mechanical properties and excellent biocompatibility, with a potential application in wound dressings [160].

BIOMEDICAL APPLICATIONS OF NANOCELLULOSE-BASED HYDROGELS

Due to their biocompatibility, biodegradability, low cytotoxicity, and excellent mechanical properties, nanocellulose-based hydrogels hold great potential for application in the biomedical field, mainly in tissue engineering, wound healing, and drug delivery.

1. Tissue Engineering

Initially, tissue engineering was proposed in 1988 as the "application of the principles and methods of engineering and life sciences toward a central understanding of the structure-function relationship in normal and pathological mammalian tissues and the development of biological substitutes for the repair or regeneration of tissue or organ function" [161,162]. Tissue engineering techniques generally require the development of exogenous 3D extracellular matrix (ECM) templates for the collection of cells in tissues, monitoring the structure of tissues, and synchronizing of cell phenotype [163,164]. In recent times, research has demonstrated that hydrogel-based biocomposites exhibit vital properties to enable the development of exceptionally effective ECMs, as well as the ability to achieve tissue proliferation cell adhesion [165]. More precisely, hydrogel scaffolds play vital roles in tissue culture as space fillers, in transporting bioactive materials, and as 3D frameworks that behave as tissue cells and prompt stimuli to monitor the development of tissue [166]. Until now, various types of natural polymers, such as hyaluronic acid and proteins, and a range of artificial polymers, including PAA, PVA, and PAAm, have been used in the formation of tissue culture frameworks [167-169]. The complex structural design of BNC fibers is very comparable to that of a biological ECM. Their spongy structure provides an environment conducive for cell growth and proliferation by ensuring adequate delivery of oxygen and nutrients across its elevated degree of interconnected pores. Due to its excellent mechanical attributes, BNC is among the most favorable potential biomaterials for use in 3D cell culture both in vitro and in organ models, and it is thought that it may even be effective in medical implants [170].

Soft tissue, such as that of the liver, muscle, blood vessels, gut, lung, nerves, articular cartilage, skin, and heart valves, performs a crucial function in the human body [171]. In our daily lives, the soft tissue in the body is destroyed as a result of trauma, disease, and aging, which generally results in non-self-reparable defects [172]. Recently, to tackle the shortcomings of different therapies, soft tissue engineering has been developed as a novel and innovative approach for fixing soft tissue wounds [173]. Biomaterial scaffolds perform a vital role in cell migration, mechanical strength support, cell remodeling, and angiogenesis [174]. So far, numerous CNCs, CNFs, and BNC-containing composite scaffolds have been developed for application in soft tissue cultures. In one study, composites based on BNC-containing poly (2-hydroxyethyl methacrylate) (PHEMA) were synthesized via the in-situ UV radical polymerization of the BNC and HEMA monomers. The findings show that the resultant composites with 10 wt% BNC exhibit enhanced mechanical capacity compared to those of pristine BNC and PHEMA hydrogels. Furthermore, biocompatibility testing showed that the prepared hydrogels are non-toxic and may offer a suitable environment for mesenchymal stem cell proliferation in mice. Consequently, the resultant composite hydrogels might be favorable biomaterial scaffolds for use in soft tissue cultures [175]. As displayed in Fig. 7(a), silk sericin (SS)-modified microstructured BNC (mBNC) composite hydrogels were synthesized and evaluated for their potential in sustaining the development of the enteric nervous system (ENS) and gut soft muscle cells (SMCs). So, it was concluded that adding SS into mBNC might stimulate proliferation and cell migration in nearby tissue to create a microenvironment that aids the redevelopment of tissue using angiogenic antioxidant properties. The obtained composite scaffolds show better growth and diversity of ENS cells and gut SMCs compared to those of pristine mBNC scaffolds. Ultimately, it was proposed that the mBNC/SS containing hydrogels might hold potential for use as scaffolds in smooth tissue engineering, such as in the blood vessels, heart, gut, and their related tissues [176]. Most recently, BCNF/gelatin/silk fibroin (SF)/reinforced composite scaffold hydrogels were synthesized via 3D bioprinting to enhance their structural and mechanical properties. The resultant hydrogels were then crosslinked using ethanol and geniposide. The treated SF/gelatin-BCNF-based composite scaffolds were then inserted beneath the skin on the dorsal side of mice to assess their biodegradability, biocompatibility, and cell permeation, the entire method of which is shown in Fig. 7(b). The study noted that a printed scaffold with 0.7 BCNF content showed high compression (65 kPa at 30% strain), with tremendous mechanical strength and self-reparability. Moreover, the in vitro and in vivo experimental results show that the composite scaffolds exhibit excellent biocompatibility and an ordered pore structure, which is beneficial for tissue growth. Thus, the resultant SF/Gelatin-BCNF scaffolds exhibit excellent potential for use in the regeneration of soft tissue [177].

Similarly, hydrogel-containing CNCs and CNFs have been extensively used in tissue cultures due to their extremely hydrated 3D spongy arrangement, which helps them to mimic biological tissue and show increased mechanical strength through the integration of the hydrogel with the CNCs or CNFs [51]. A high internal phase emulsion (HIPE) synthesized using 2-ureido-4[1H]-pyrimidone (UPy)-treated CNCs (CNC-UPy) as Pickering stabilizers has been developed, with the results indicating that HIPE might be useful as a prototype to produce hybrid macroporous hydrogels. Therefore, it was concluded that by adjusting the concentration of CNC-UPy, the swelling actions, spongy structures, and mechanical strength of the obtained hybrid macroporous hydrogel could be controlled. Also, the hybrid hydrogels showed outstanding cell adhesion and cytocompatibility. Thus, it was assumed that the resultant hybrid hydrogels are potential candidates for use in tissue engineering [178]. In another study, a lightweight and highly porous artificial bone template was synthesized by the fabrication of in situ hydroxyapatite (HAP) in the matrix of CNCs, supported via a crosslinking mechanism. The outcome revealed that the mechanical strength (up to 41.8 MPa) and water stability of the CNC/HAP scaffolds are considerably improved as a result of crosslinking with PEG and poly (methyl vinyl ether-alt-maleic acid) (PMVEMA). Also,

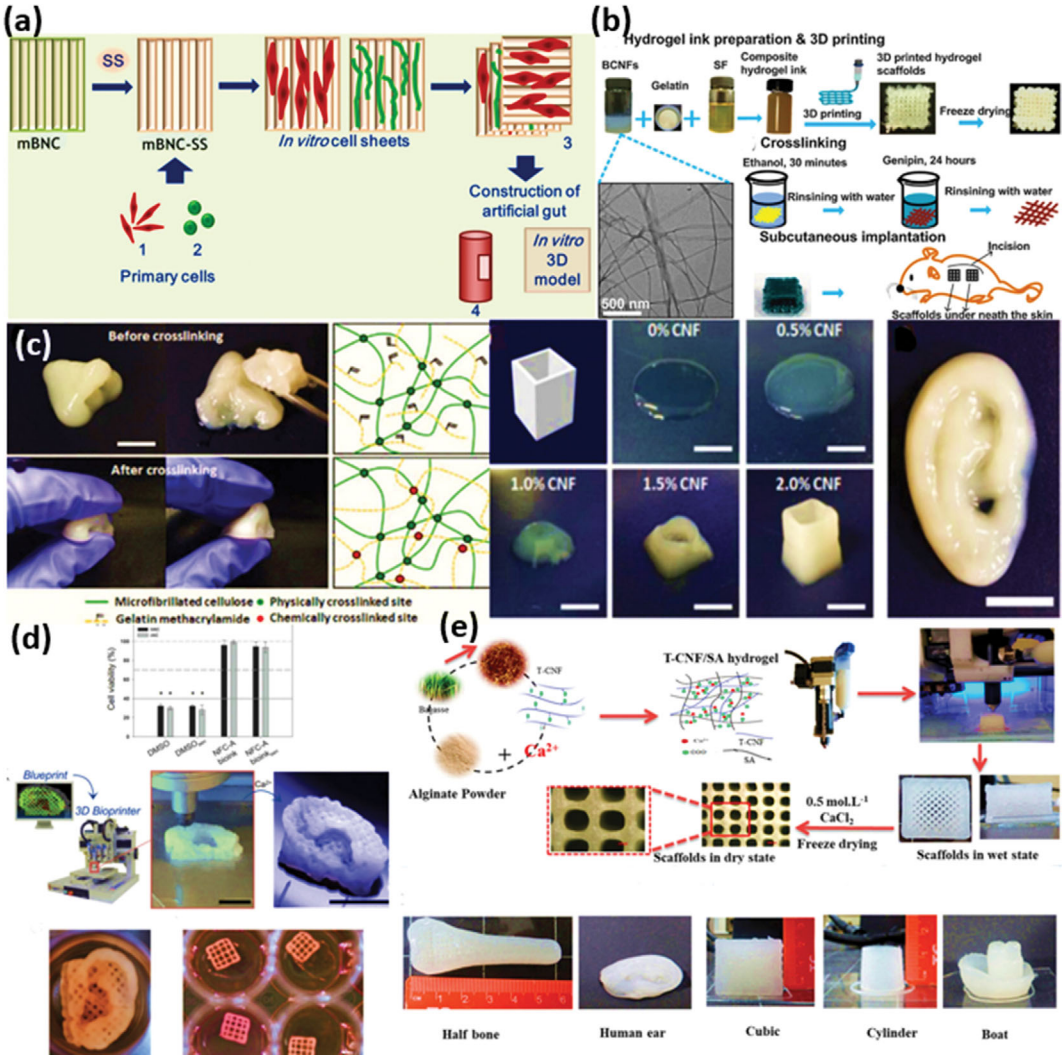

Fig. 7. (a) Proposed design for mimicking the gut wall via layer-by-layer construction using microstructured bacterial nanocellulose-silk sericin scaffolds [176], reproduced with copyright permission from Elsevier; (b) graphical interpretation of the synthesis of silk fibroin/gelatin-bacterial cellulose nanofiber hydrogel scaffolds and their subcutaneous implantation [177], reproduced with copyright permission from Elsevier; (c) illustration of the rheological properties and printability of gelatin methacrylamide/cellulose nanofibril composite inks [136]; (d) three-dimensional (3D) bioprinting of chondrocyte-laden NFC-A auricular constructs with open porosity [187], reproduced with copyright permission from Elsevier; and (e) fabrication method for the 3D bioprinting of scaffolds from T-CNF/sodium alginate hydrogels along with scaffolds of various forms and shapes printed using the optimal hydrogel preparation [188], adapted with copyright permission from the American Chemical Society.

the composite scaffolds exhibit excellent biocompatibility, with the capacity for stabilizing bovine serum albumin (BSA) protein. The results suggest that the resultant composites are favorable candidates to act as bone scaffolds [179].

Nowadays, injectable CNF- and CNC-based hydrogels receive much research attention due to being injectable into precise locations and capable of being incorporated into unusual defects in materials [178]. For instance, in a study on the development of injectable carboxymethyl cellulose (CMC)/dextran-based hydrogels reinforced with aldehyde-functionalized CNCs (CHO-CNCs), it was revealed that the CNC crosslinked hydrogels show superior elastic moduli (around 140% surge peak intensity) and better dimensional stability in prolonged (60 days) swelling tests compared to the pure hydrogel. No considerable cytotoxicity to NIH 3T3 fibroblast cells was detected in the prepared hydrogels. It was indicated that such types of injectable hydrogels might be used in templates for the regeneration of tissue [180].

Recently, 3D bioprinting has been used to develop CNC-, CNF-, and BNC-containing hydrogels with 3D molded shapes for use in tissue culture frameworks [181-183]. These 3D-shaped frameworks show excellent potential for the renewal of tissue, as well as the repairing and replacing of organs [136,184]. The BNC/PCL composite templates have been effectively synthesized using the EHD 3D bioprinting technique. The typical fiber size of the BNC/PCL composite framework was 100 μm and the depth size of the fibers was 4.7±1.03 μm. The composite scaffolds displayed improved bio-

compatibility and enabled cellular proliferation and were applied in an additional study for the delivery of growth drugs to assist in the development of tissues in skin tissue engineering applications. A green ink printed bio-composite, containing TEMPO-oxidized bacterial cellulose (TOBNC), laponite nano clay (Xls), and SA, has been synthesized. This 3D bioprinted ink not only shows mechanical strength but also long-lasting performance in the delivery of protein, meaning that it is a potential candidate for use in tissue engineering [185].

A biomimetic ink comprising CNFs as a reinforcing material, crosslinked with a xylan-based matrix, has been developed and used in the 3D bioprinting of scaffolds. Researchers have indicated that the resultant 3D-printed composite hydrogels exhibit promising applications in tissue cultures, as bio-ink easily forms a gel with high water content. Another 3D printable bio-ink composite has been synthesized containing CNFs and gelatin methacrylamide (GelMA). As shown in Fig. 7(c), using a bio-ink of GelMA/CNFs, a structure of the human nose was effectively printed, although the printed hydrogel was demolished due to only physical crosslinking regions (e.g., intermolecular hydrogen bonding and the entanglement of fibers) being present among the CNFs. After crosslinking with GelMA and achieving the formation of chemical covalent bonds using an APS/TEMED initiator approach, the printed hydrogel of the human nose developed a diffuse structure and, as a result, became a material with a highly elastic and mechanically stable network [136]. Another bio-ink containing CNF with outstanding shear-thinning attributes and featuring alginate that exhibits a fast-crosslinking capacity has been synthesized for the 3D bioprinting of living soft tissue with cells. The printability of this material was studied, in terms of its rheology, shape distortion, and compression, and it was discovered that Ink 8020, which contains 20% alginate and 80% CNFs by weight, exhibits good gelation properties during crosslinking and a slight propensity for shape distortion [186]. Furthermore, human chondrocytes have been bioprinted in a non-cytotoxic CNF-containing hydrogel, which showed 73% and 86% cell sustainability after one and seven days of 3D culturing, respectively. It was shown that the CNF-containing bio-ink hydrogel is more favorable for 3D bioprinting involving living cells. Soon after, a bio-ink related to Ink8020, referred to as NFC-A bio-ink, was synthesized for the tissue engineering of auricular cartilage, in the 3D bioprinting of a human ear, as shown in Fig. 7(d). It was noted that the patient sported an ear of exceptional shape and size after its bioprinting and 3D culturing for up to 28 days. Moreover, human nasal chondrocytes (hNC) have been shown to grow and undergo chondrogenesis via 3D culturing in NFC-A bio-ink, which was used in neo-synthesis and the assembling of cartilage-specific extracellular matrices across cells. The outcome of this study showed that NFC-A might be a potential bio-ink for use in the regeneration of auricular cartilage tissue [187].

In recent times, as illustrated in Fig. 7(e), a T-CNF/SA-based biomimetic 3D-printed hydrogel has been synthesized via extrusion-based 3D bioprinting and crosslinked using Ca^{2+} calcium ions with distinct factions. It was concluded that bio-ink with 50% alginate and 50% T-CNFs showed the best printability and highest reliability in the replication of the digital item. Similarly, the T-CNF/SA-based hydrogel exhibited outstanding mechanical attributes in comparison to pristine SA- and T-CNF-containing hydrogels. Furthermore, hydroxyapatite biomimetic mineralization was reported and the estimated quantity of hydroxyapatite in the mineralized templates was assessed as 20.1%. It was assumed that T-CNF/SA mineralized-based hydrogel scaffolds might be a potential material for use in the regeneration of bone tissue [188].

2. Wound Healing

Human skin acts as a body shield and executes many critical functions, such as body temperature monitoring, balancing of electrolytes and water, and sense of feeling. In everyday life, skin injuries occur that require proper treatment for the prevention of further deep-rooted injuries and to promote smooth healing [189]. Wound dressing can be used as an easy and efficacious method for repairing skin wounds. However, some requirements need to be met for a material to be considered as an "ideal" wound dressing material. An ideal wound dressing material must be non-contaminated and non-allergenic, with a capacity for being able to survive the humidity at the surface of a wound, show good absorbency to gases, show antimicrobial activity, absorb extra transude and contaminants, promote healing, suppress additional inflammation, and must be easily detachable without causing any additional damage to the wound [190]. The CNC-, CNF-, and BNC-based hydrogels mostly meet the aforementioned requirements and have thus received much research attention over the last few years for use in wound dressing. For instance, CNF-reinforced hydrogels have been developed for wound healing applications. Using various types of hemicellulose (xyloglucan [XG], xylan, and galactoglucomannan [GGM]) as crosslinkers at various weight percentages, the mechanical and structural attributes of hydrogel scaffolds can be modified. Then, the impact of these modified features on cellular performance during wound healing was examined. It was discovered that XG shows the maximum capacity for adsorption on the CNFs, which tend to impart the best reinforcement effect and help in the proliferation of NIH 3T3 cells. These complex hydrogels exhibit favorable capability in wound recovery applications to support networks and to stimulate cell adherence, development, and proliferation [191]. As displayed in Fig. 8(a), an injectable hydrogel has been synthesized that contains dialdehyde-modified CNCs and carboxymethyl chitosan to heal intense burn wounds. Intriguingly, the hydrogel can be removed when needed using a solution of an amino acid, which helps to accelerate the healing process and eradicate pain when the wound dressing is being changed, along with preventing the formation of scars [192].

Metal and metal oxide nanoparticles (MNPs/MONPs), such as Ag, CuO, Cu, ZnO, TiO_2, MgO, and Fe_3O_4 NPs, have antimicrobial characteristics that promote wound healing. Therefore, metal oxide-based cellulose nanomaterials have been extensively studied. In recent work, BNC/ZnO nanocomposites have been synthesized and the capacity of an as-synthesized BNC/ZnO-based material was assessed for the treatment of burn abrasions. The antimicrobial activity of the BNC/ZnO-containing material was analyzed against conventional burn pathogens, with the outcomes revealing that the resultant material shows outstanding antibacterial action against *E. coli*, *Citrobacter freundii*, *S. aureus*, and *P. aeruginosa*. Furthermore, in vivo studies on burn mice models were performed to check the wound treatment capability of the BNC/ZnO nanocom-

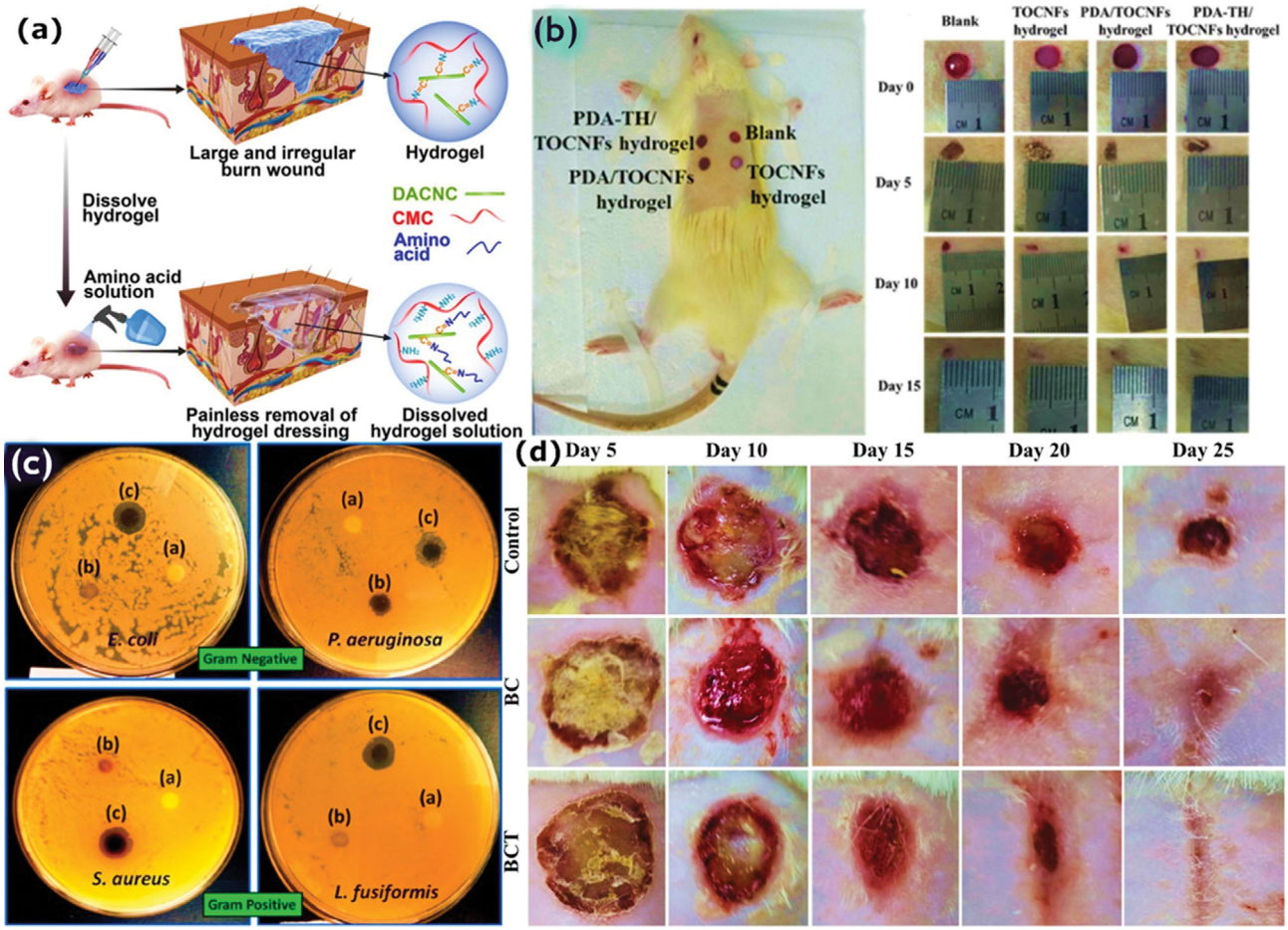

Fig. 8. (a) Flow chart showing on-demand dissolvable self-healing hydrogels for deep partial-thickness burn wound healing [192], adapted with copyright permission from the American Chemical Society; (b) schematic diagram of the wound healing of different groups healed with TOCNF, phenylene diamine (PDA)/TOCNF, and PDA–TH/TOCNF hydrogels [199], reproduced with copyright permission from Elsevier; (c) study of the antimicrobial activity of CM-bacterial cellulose (BNC), BNC–dopamine, and BNC-DOPA/reduced graphene oxide/Ag NP films against Gram-negative (*E. coli* and *P. aeruginosa*) and Gram-positive (*S. aureus* and *L. fusiformis*) bacteria [200], adapted with copyright permission from the American Chemical Society; and (d) representative images of burn wounds in control, BNC, and thymol bacterial nanocellulose groups at days 5, 10, 5, 20, and 25 [201], reproduced with copyright permission from Elsevier.

posite material. It was found that the resultant nanocomposite demonstrates better healing activity (66%) than that of the pure BNC material [193]. In another study, BNC/TiO_2-containing nanocomposite aerogel scaffolds were developed and their applicability for burn wound recovery was examined. The results revealed that the synthesized BNC/TiO_2 nanocomposites show inhibitions of 83% and 81% against *S. aureus* and *E. coli*, respectively. In vivo results show that the resultant nanocomposites display exceptional therapeutic capability, with fast wound reduction capability and rapid re-epithelization percentage, implying that BNC/TiO_2 might be an excellent material for the treatment of burn wounds [194].

Most recently, a green nanocomposite has been synthesized from amine silver nanoparticles (Ag-NH_2 NPs) and gelatin-based TOCNFs. The results show that hydrogel patches with 0.5 mg/mL of Ag-NH_2 NPs (CNF/gelatin/Ag0.5) reveal excellent self-healing, strong mechanical and antibacterial properties, reasonable hemostatic ability, and suitable moisture content when applied to a wound. From an in vivo wound repairing experiment, it was found that a CNF/gelatin/Ag0.5 composite hydrogel dressing exhibited better efficiency of around 90% in the wound healing along with an 83.3% chance of existence after 14 days [195]. Likewise, BNC/AgNP composite hydrogels have been synthesized to study their wound repairing capability. The results exhibit that the resultant composites show pronounced antibacterial action against *S. aureus*. Moreover, the impact of the resultant hydrogels on cell evolution was analyzed in the in vitro experiments. The results revealed that the resultant hydrogels exhibited minimal cytotoxicity against rat fibroblasts. It was concluded that the depth of stimulated dermis and epidermal beneath the obtained hydrogels was greater than that beneath pristine BNC. Consequently, it was concluded that this type of BNC/AgNP hydrogel might be an excellent material for use in antimicrobial wound dressings [196].

Recently, CNF-based hydrogels have been synthesized by utilizing the metal cationic crosslinking method for wound dressing applications. These types of hydrogels have received much research attention due to their simple processing and tunable mechanical

properties. For instance, TOCNF hydrogels with cross-links formed using calcium ions have been synthesized as promising materials for use in wound dressing applications. It was found that the as-prepared hydrogels can withstand humidity and exhibit mechanical stability. Moreover, the hydrogels did not disturb the monolayer culture of dermal fibroblasts upon direct interaction with them and displayed static behavior in the case of the swell ability reaction with mononuclear cells. These findings emphasize the excellent capability of ion crosslinked TOCNF hydrogels in the design of innovative wound dressing materials. The impact of crosslinking agents (Ca^{2+} or Cu^{2+}) on the antibacterial properties of the hydrogels against various types of bacterial species was explored. The results demonstrate that the calcium ion-crosslinked TOCNF hydrogel hindered the settlement of *Staphylococcus* epidermidis and stopped the formation of biofilm of *Pseudomonas aeruginosa*, whereas the copper ion-crosslinked TOCNF hydrogel prohibited the growth of *Staphylococcus* epidermidis and developed *P. aeruginosa* to static condition [197]. Hence, the further design of innovative wound dressings, along with the regulation of antibacterial properties, might be achieved using various types of crosslinking agents. To date, 3D-printed CNF hydrogel scaffolds have been fabricated that exhibit tunable mechanical properties, synthesized via the crosslinking of TOCNFs with calcium ions by in situ polymerization and after-printing crosslinking with 1,4-butanediol diglycidyl ether. It was discovered that the mechanical properties of the as-synthesized 3D-printed CNF-based hydrogel might be tunable on a scale of 3-8 kPa. Furthermore, the in vivo findings showed that the synthesized CNF hydrogel templates present no hazard to fibroblast cells. Besides this, the 3D bioprinted arrangement of the hydrogel templates improved the ability of the created matrix to boost cell proliferation, which is crucial in generating a material that rapidly repairs lesions [198]. In an alternative study, unique multi-receptive-based tetracycline hydrochloride (TH) complex TOCNF hydrogel filled with polydopamine (PDA) and crosslinked with calcium ions was synthesized that exhibits drug delivery and wound repair properties. Hence, it was discovered that TH might be discharged from the synthesized hydrogel when required under the influence of near-infrared irradiation or at lower pH. As shown in Fig. 8(b), in vivo skin flaw tests demonstrated that the synthesized composite hydrogel shows outstanding wound repairing properties [199].

Recently, a novel antibacterial dopamine (DOPA)-based BNC-DOPA/rGO/AgNP transdermic dressing has been synthesized for use in abrasion repairing applications. As shown in Fig. 8(c), the resultant composite dressing shows exceptional antibacterial capability against Gram-negative and Gram-positive bacteria in comparison to pristine BNC. Furthermore, a survey of the cytotoxicity of the BNC-DOPA/rGO/AgNPs showed that the attained composite dressing is congruent with the NIH 3T3 cell line. Likewise, expedited proliferation and relocation of both A549 human lung epithelial cells and NIH 3T3 fibroblast cells were observed with the resultant composite dressing treated group, showing outstanding wound repairing performance. Hence, the synthesized mussel biomimetic BNC-DOPA/rGO/AgNP transdermal dressing system shows excellent properties for use in the repairing of abrasions [200].

Note that there are polymers that exhibit outstanding antibacterial properties. For example, thymol, which is extracted from plants such as thyme, is a natural essential oil component that displays excellent antibacterial activity against contagious bacteria, showing anti-inflammatory properties [196]. Recently, the fabrication of thymol-improved BNC hydrogels (BNCT) was reported, with an assessment of their applicability in the repairing of burn wounds. The antimicrobial results of this study suggest that the acquired BNCT hydrogels show excellent biocidal activity against burn pathogens. Also, an in vitro study showed that the BNCT-containing hydrogels exhibit low toxicity and proficiently accelerate fibroblast cell evolution. In vivo analysis was performed in female rats to assess the wound repairing activity of the resultant composite hydrogels. As shown in Fig. 8(d), compared to the pristine BNC groups, significantly improved healing (90.7%) was exhibited on day 20, and almost complete healing was observed on day 25 in the BNCT group. The findings show that the BNCT-containing hydrogels are appropriate for use as natural burn wound repairing materials [201]. Lignin is deemed to be the most prevalent aromatic biopolymer on earth [202]. It has been revealed in numerous studies that lignin and its byproducts display excellent antibacterial activities, as showing promise as materials for antibiotics [203,204]. Similarly, BNC/COL-based composite hydrogels have been synthesized to screen the healing capacity of wounds in rats. The results reveal that the resultant hydrogels exhibit good characteristics in a moist environment and adhere to wounds very easily. Thus, the resultant hydrogels act as potential dressings for wound healing [205]. Likewise, dextran, which consists of glucose subunits, has been potentially utilized for abrasion healing due to its excellent biological attributes [206].

Recently, several excellent wound repairing hydrogels have been synthesized by integrating synthetic polymers, such as PAA and PAAm, with a BNC hydrogel. For instance, BNC/PAAm-containing composite hydrogels show a specific resemblance to natural smooth tissue, and their applicability in burn wound dressing has been examined in numerous studies [207]. BNC/PAAm-containing composite hydrogels have been synthesized using microwave irradiation that exhibits good swelling behavior and high porosity. The resultant composite hydrogels were additionally evaluated in the healing of partial burn wounds. Also, it was revealed that the resultant hydrogels stimulate fibroblast proliferation and regenerative epithelialization and speed up the repairing process of wounds [208]. Likewise, PAA is a popular ionic polymer having chains of ionic groups, which has revealed pH-responsive properties [209]. A pH-responsive BNC/PAA composite hydrogel has been synthesized via the grafting of amoxicillin on a hydrogel for drug discharge. It was found that the resultant hydrogel shows pH-responsive behavior in terms of both drug release and swelling properties. The hydrogel showed adsorption of excess exudate and the delivery of large amounts of drug at elevated pH, which implies that it might be appropriate for use in chronic wound repairing [210]. Later, BNC/PAA composite hydrogels were prepared using an electron beam irradiation method. Human epidermal keratinocytes (HEKs) and human dermal fibroblasts (HDFs) were filled into the resultant hydrogels and their ability to heal wounds was analyzed in athymic mice. The resultant-loaded hydrogel cells showed a 77.3% wound lessening rate after 13 days that was much

greater than that of the control group (around 64.8%). Hence, it was shown that the resultant hydrogels act as promising materials and cellular transporters in the rapid healing of wounds [211]. Later, the same group thoroughly evaluated the capability of BNC-containing PAA hydrogels to distribute HEKs and HDFs for the treatment of skin abrasions. Furthermore, an in vivo study revealed that the resultant hydrogels filled with cells (HC) demonstrated excellent abrasion healing ability in contrast to hydrogels alone (HA). The results show that the HC group demonstrates promising healing capability [212]. The outcomes of the study show that the resultant composite hydrogels have the dual functionality of wound dressing and cell carrier properties to stimulate the healing of thick wounds.

3. Drug Delivery

The CNCs, CNFs, and BNCs act as potential carriers of bioactive materials for the application of drug delivery due to their extraordinary nanostructures, biodegradability, biocompatibility, and regulated surface chemistry [213,214]. Moreover, due to their high surface areas and open-pore structures, CNC-, CNF-, and BNC-based hydrogels may show better bioavailability and superior drug loading capability. Therefore, in recent years, a variety of drug-releasing hydrogels containing CNCs, CNFs, and BNC have been synthesized [215]. In one study, spongy collagen/CNCs scaffolds integrated with recyclable gelatin microspheres (GMs) have been reported comprising primitive fibroblast growth factor (bFGF) for long-term delivery and subsequent improvement in angiogenic capability. It was observed that at 5 wt% CNC concentration, the composite scaffold showed supreme swelling capability, and the GMs/bFGF-integrated scaffolds enhanced the number of freshly developed and matured blood vessels. Likewise, a CNC/starch hydrogel has been developed and explored for vitamin B12 discharge. The findings of this study revealed that the CNC/starch fabricated hydrogel shows a roughly 2.9-times slower delivery rate than starch-containing microgels as CNCs prevent drug discharge [216]. Furthermore, a double membrane hydrogel system has been prepared from cationic CCNCs and anionic alginate for the co-delivery of drugs. In the outer region of the material, the anionic alginate hydrogel promotes the rapid release of drugs, over three days, whereas the inner region of the membrane with the CCNC hydrogel causes a delay in the releasing of the drug from four to 12 days. Consequently, the dual-layer hydrogel was responsible to provide resistance in the delivery of drugs and is projected to show synergistic effects in biomedical applications [217]. Recently, magnetic CNC/alginate beads have been reported for use in drug delivery. In this study, it was observed that the presence of magnetic CNCs in the material enhances the reliability of the beads and their rate of swelling [218]. The impact of the presence of CNCs in PAA-chitosan nanoparticles in PVA hydrogel contact lenses to control the ophthalmic drug release has been examined. It was noted that the integrated CNC-PVA lenses exhibit improved release potential compared with lenses without CNCs. This occurs due to the gelation of the nanoparticles as well as the presence of the CNCs immobilized in the PVA gel network, which inhibits leakage via the intertwining of the PVA particles with the CNCs. Hence, it is thought that innovative precise drug discharge ocular lenses can be developed by blending them with functional CNCs [219]. CNF-based hydrogels have also been explored for use in drug release systems. An injectable technetium-99 m-labeled CNF-based hydrogel was developed for in vivo drug delivery, which allows the tracing of the site of the CNFs hydrogels and the assessment of the in vivo delivery of the drug. It was shown that the synthesized CNF hydrogels act as a template for the restricted and regional release of macro compounds. Remarkably, the CNF-based hydrogels, which are harmless and biocompatible, might be broken down into glucose by cellulose processing enzymes [220]. In a further study, the impact that freeze-drying and successive rehydration have on the rheological properties and drug delivery applications of TOCNF hydrogels was explored. It was observed that freeze-dried CNF hydrogels could be easily re-dispersed without having any impact on their drug delivery properties. Hence, the TOCNF hydrogels can be stored in a dry state and only re-dispersed when required, which is beneficial for real-time clinical applications [221].

In recent years, stimuli-responsive CNF-based hydrogels have received a significant amount of interest, due to their capability to release drugs in the presence of stimuli (e.g., ionic strength, pH, and temperature), when required. For instance, the synthesis of dual-responsive TOCNF/PNIPAM-containing composites for drug delivery has been reported. It was observed that the pH-responsive traits of the CNF/PNIPAM hydrogels might be developed by regulating the charge on the carboxylic groups of the CNFs. It was found that the swelling percentage of the composite could be additionally adjusted by changing the temperature. Later, the synthesis of a pH-responsive macrosphere gel containing TOCNFs and SA using $CaCl_2$ as a cross-linker was reported. It was revealed that the as-prepared macrosphere gel plays an excellent role in gastric juice, improving the shielding of fabricated probiotics in an acidic medium in the body. Moreover, it able to swell in intestinal fluid, resulting in the discharge of the fabricated probiotics [222]. Consequently, the assembled macrosphere gel exhibited excellent functioning in the intestinal-targeted release of probiotics. After this study, the fabrication of bio-inspired microcapsules based on xyloglucan (XyG), pectin from apple (AP), and cationic CNFs was prepared via an LbL method. It was revealed that the microcapsules display (ON/OFF) stimuli-responsive penetrability and biocompatibility. Similarly, living cell staining research has shown that harmless microcapsules boost cell progression. Ultimately, it was predicted that the microcapsules hold great potential for use in bioactive applications, for instance, their colon-targeted release in the gastrointestinal region of the body [223].

Recently, BNC-containing hydrogels were thoroughly examined as a drug release system for albumin protein templates. In this study, it was observed that the stacking and release of protein follows a typical polymer-based hydrogel method, i.e., a diffusion and swelling-controlled system. Likewise, it was discovered that a freeze-dried BNC aerogel showed a lower drug filling capability than a regional BNC hydrogel owing to the alteration in the network of the BNC nanofibers. The potential of BNC templates was assessed to determine their oral drug release (e.g., tizanidine, famotidine) properties. The BNC templates were shown to have better drug delivery properties than the native tablet dosage in their freeze-dried, hydrated, and partially hydrated states [224]. The synthesis of BNC-containing capsule shells for the well-regulated delivery of

oral drugs has been reported and it was revealed that pristine BNC capsules show rapid drug discharge capacity that may be prolonged via the insertion of delivery-blocking cellulosic material (e.g., CMC, hydroxypropyl methylcellulose) into pristine BNC capsules. The impact that the surface alteration of BNC has on drug insertion and the discharge abilities of the affected oral drugs was explored. The findings suggest that the improved BNC shows the persistent release of drugs. Therefore, surface modification might be an efficient approach by which to control the drug delivery characteristics of BNC hydrogels [225]. The logical design of BNC composites for rapid and extremely effective drug release has drawn significant research attention. Later, the homogeneous insertion of graphene oxide (GO) into a 3D spongy BNC network using an in-situ biosynthesis system was developed, as a unique approach for the release of ibuprofen (IBU). It was revealed that the existence of GO in the hydrogel complex boosts the stacking of IBU due to its improved surface area. Fig. 9(a) shows the proposed interaction of BNC/GO hydrogels and IBU, via hydrogen bonding interactions, where it is thought that IBU adsorbs on both sides of GO and BNC. The drug delivery performance of the BNC/GO hydrogels suggests that the rate of drug delivery is higher under neutral conditions than under acidic conditions, with the resultant composite exhibiting a much-sustained discharge performance than that of IBU@BNC. Moreover, the BNC/GO-containing composite hydrogels exhibit excellent cell sustainability compared to pristine BNC hydrogels. Consequently, these novel BNC/GO nano carriers might be a good candidate for drug release [226]. In an additional study, BNC/gelatin copolymers crosslinked with glutaraldehyde were synthesized. The results of this study revealed that the copolymers showed improved chemical and mechanical properties owing to the formation of hydrogen bonds between the -OH groups of the BNC and the -NH_3 groups of the gelatin. Remarkably, the copolymers displayed 400%-600% expansion in water. The resultant BNC/gelatin copolymers exhibited a thicker structure than their pristine counterpart, which led to them showing a persistent drug discharge profile, indicating that they hold the potential to produce regulated drug release systems [227].

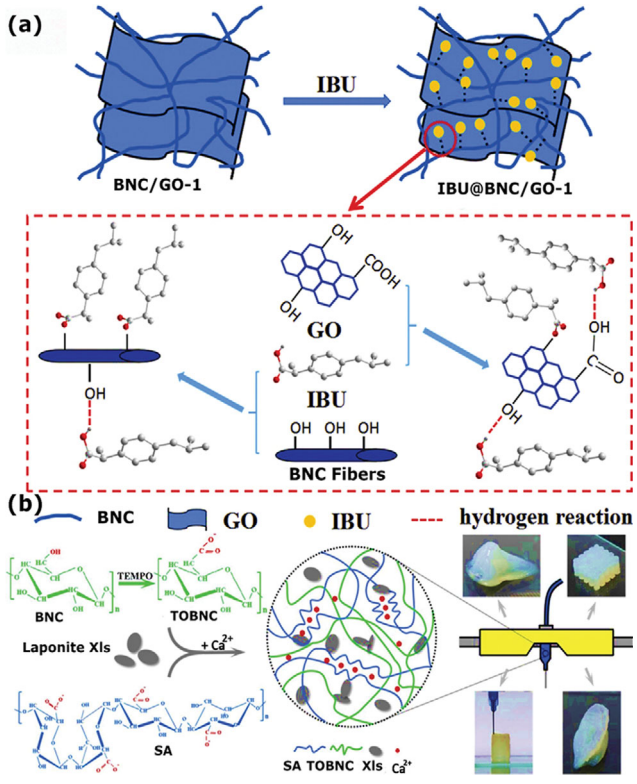

Fig. 9. Schematic overview of the synthesis and drug delivery approach: (a) the mechanism of the surface interactions between bacterial cellulose/oxidized graphene and ibuprofen [226], reproduced with copyright permission from Elsevier and (b) schematic diagram of the fabrication of the hydrogel for drug delivery [228], reproduced with copyright permission from Elsevier.

Recently, a TOBNC/SA/Xls 3D-bioprinted ink nanocomposite was prepared, which displays excellent printability compared to TOBNC/SA, as shown in Fig. 9(b). The resultant 3D-printed ink shows good persistent protein release behavior, demonstrating carrying, protecting, and release properties for tissue engineering. Moreover, the obtained 3D-printed ink nanocomposite shows structural stability in phosphate-buffered saline for more than 14 days, and with 0.5% Xls content provides excellent support for cell propagation, which is favorable for tissue growth and replacement. It was thus concluded that the as-prepared 3D-printed TOBNC/SA/Xls hydrogel exhibits excellent drug delivery properties [228].

SUMMARY AND OUTLOOK

Over the past few decades, cellulose has been widely used as a biomaterial in biomedical applications due to its sustainability, biodegradability, and biocompatibility. In this review, different plant sources of cellulose and its percentage content have been discussed. As mentioned, from a morphological perspective there are two types of cellulose structures, CNC and CNFs. Cellulose can also be obtained from bacteria, referred to as bacterial cellulose. From the information presented in this review, it can be concluded that CNFs form a more stable mechanical hydrogel on their own than CNCs as CNFs have a high aspect ratio that leads to them having an entangled and interwoven network. In contrast, the CNCs have a rigid structure with a low aspect ratio. Likewise, pure BNC scaffolds also have certain shortcomings, such as uncertain mechanical properties and a lack of antibacterial activity. These shortcomings restrict their use in some biomedical applications, such as in wound dressings, which require materials to have antibacterial properties, and tissue engineering scaffolds, in which good mechanical strength is essential. However, these defects of BNC can be improved through interaction with various nanoparticles, and synthetic and natural polymers, due to their unique nanostructures, superior mechanical properties, and highly reactive surfaces, as well as biodegradability, and biocompatibility.

In this review, traditional as well as emerging approaches for the preparation of hydrogels are discussed, such as 3D bioprinting, and their types and potential applications in the biomedical field have been summarized, with a particular focus on tissue engineering, wound dressings, and drug delivery scaffold applications. To date, only limited clinical trials have been performed on an in

vitro level. For instance, CNF-based hydrogel wound dressings have been tested in trials on burn patients to explore their promising behavior in the healing of wounds. The results of these trials show that no inflammatory and allergic reactions were observed. Furthermore, from long-term toxicological studies, it was observed that CNC-, CNF-, and BNC-based hydrogel scaffolds did not have any dangerous effects on targeted tissues or organs; however, large-scale production and clinical trial data are still limited due to the in vivo degradability of nanocellulose-based scaffolds which remains a challenge as nanocellulose itself does not completely degrade in the human body due to the lack of relevant enzymes [229,230]. This issue must be tackled because the breakdown of a constructed scaffold after implantation is crucial in order to improve the interaction between host tissues and those encapsulated in the scaffold. Especially, the most captivating question for material scientists in basic research is how to chemically modify or engineer nanocellulose materials to make them self-degrade naturally in the human body. Despite the limitations, a variety of nanocellulose based 3D bio-inks have been developed commercially i.e., UPM-Kymmene Corporation has recently introduced a medical-grade CNF hydrogel with the logo of GrowInkTM as a vegan-derived bio-ink, as well as a CNF-based wound dressing product of FibDex® for the European market. As confirmed in a clinical trial of a small group of patients, FibDex® is alleged to provide a beneficial environment for wound healing [231]. Swedish bioprinter supplier CELLINK is also commercializing CNF/alginate bio-inks as accessory kits for the use in their bioprinter series. Their CNF/alginate bio-ink was used to fabricate human cartilage structure with chondrocytes and stem cells co-cultured inside the hydrogel. As assessed in an in vivo mice model, the matrix favored not only the proliferation of chondrocytes but also the secretion of glycosaminoglycans and collagen II by the chondrocytes [232].

Overall, 3D bioprinting is a technique that can produce CNC-, CNF-, and BNC-based hydrogels having tailored hierarchical structures and provide a promising route to allow these hydrogels to be produced on a large scale and support the further development of potential biomedical products. It is hoped that this review will provide the impetus to develop more CNC-, CNF-, and BNC-based scaffold hydrogels for use in various biomedical applications in the future.

ACKNOWLEDGEMENTS

The authors are very grateful for financial support from the Ministry of Trade, Industry & Energy of the Republic of Korea (20014762) and the National Research Foundation of Korea (Grant No. 20201I1A304491).

NOMENCLATURE

Abbreviated Name

AA	: acrylic acid
APS	: ammonium persulfate
BNC	: bacterial cellulose
BNC/COL	: collagen-based bacterial nanocellulose
BCNC	: bacterial cellulose nanocrystals
BCNF	: bacterial cellulose nanofibers
BNCT	: thymol bacterial nanocellulose
bFGF	: fibroblast growth factor
BSA	: bovine serum albumin
cCNC	: carboxylate cellulose nanocrystals
CCNC	: cationic cellulose nanocrystals
CHO-CNC	: aldehyde-based cellulose nanocrystals
CMC	: carboxymethyl cellulose
CNC	: cellulose nanocrystals
CNF	: cellulose nanofibrils
CS	: chitosan
chCNFs	: chitin nanofibers
DOPA	: dopamine
ECMS	: extracellular matrix system
ENS	: enteric nervous system
G	: graphene
GelMa	: gelatin methacrylamide
GGM	: galactoglucomannan
GMs	: gelatin microspheres
GO	: oxidized graphene
HA	: hydrogel alone
HAP	: hydroxyapatite
HC	: hydrogel filled with cells
HEMA	: 2-hydroxyethyl methacrylate
HIPE	: high internal phase emulsion
hNC	: human nasal chondrocytes
IBU	: ibuprofen
LbL	: layer-by-layer
m(BNC)	: microstructured bacterial nanocellulose
MDI	: methylene diphenyl diisocyanate
MNPs	: metal nanoparticles
MONPs	: metal oxide nanoparticles
PAA	: poly(acrylic acid)
PAAm	: polyacrylamide
PBS	: phosphate-buffered saline
PDA	: phenylenediamine
PEG	: polyethylene glycol
PEGDA	: poly(ethylene glycol) diacrylate
PHEMA	: poly(hydroxyethyl methacrylate)
PNIPAAM	: poly(*N*-isopropyl acrylamide)
PMVEMA	: poly(methyl vinyl ether-alt-maleic acid)
rGO	: reduced graphene oxide
SA	: sodium alginate
Semi-IPN	: semi-interpenetrating network
SF	: silk fibroin
SL	: stereolithography
SMCs	: soft muscle cells
SS	: silk sericin
TEA	: triethylamine
TEMED	: *N*, *N*, *N*′, *N*′-tetramethylethylenediamine
TEMPO	: (2,2,6,6-tetramethylpiperidin-1-yl) oxyl
TiO_2	: titanium dioxide
UPy	: 2-ureido-4[1H] pyrimidinone
Xls	: laponite mono clay
XyG, XG	: xyloglucan
ZnO	: zinc oxide

REFERENCES

1. Y. Habibi, L. A. Lucia and O. J. Rojas, *Chem. Rev.*, **110**, 3479 (2010).
2. P. Gatenholm and D. Klemm, *MRS Bull.*, **35**, 208 (2010).
3. S. J. Eichhorn, A. Dufresne, M. Aranguren, N. E. Marcovich, J. R. Capadona, S. J. Rowan, C. Weder, W. Thielemans, M. Roman, S. Renneckar, W. Gindl, S. Veigel, J. Keckes, H. Yano, K. Abe, M. Nogi, A. N. Nakagaito, A. Mangalam, J. Simonsen, A. S. Benight, A. Bismarck, L. A. Berglund and T. Peijs, *J. Mater. Sci.*, **45**, 1 (2010).
4. S. Kalia, A. Dufresne, B. Mathew Cherian, B. S. Kaith, L. Avérous, J. Njuguna and E. Nassiopoulos, *Int. J. Polym. Sci.*, **2011**, 837875 (2011).
5. E. Kalita, B. K. Nath, P. Deb, F. Agan, M. R. Islam and K. Saikia, *Carbohydr. Polym.*, **122**, 308 (2014).
6. T. Saito, R. Kuramae, J. Wohlert, L. A. Berglund and A. Isogai, *Biomacromolecules*, **14**, 248 (2013).
7. G. L. Louis and B. A. K. Andrews, *Text. Res. J.*, **57**, 339 (1987).
8. N. Rehman, S. Alam, N. U. Amin, I. Mian and H. Ullah, *Int. J. Polym. Sci.*, **2018**, 8381501 (2018).
9. A. K. Bledzki, A. A. Mamun, M. Lucka-Gabor and V. S. Gutowski, *Express Polym. Lett.*, **2**, 413 (2008).
10. M. M. Ibrahim, W. K. El-Zawawy, Y. Jüttke, A. Koschella and T. Heinze, *Cellulose*, **20**, 2403 (2013).
11. J. I. Morán, V. A. Alvarez, V. P. Cyras, and A. Vázquez, *Cellulose*, **15**, 149 (2008).
12. A. Thygesen, J. Oddershede, H. Lilholt, A. B. Thomsen and K. Ståhl, *Cellulose*, **12**, 563 (2005).
13. Y. Habibi, *Chem. Soc. Rev.*, **43**, 1519 (2014).
14. C. Somerville, *Annu. Rev. Cell Dev. Biol.*, **22**, 53 (2006).
15. F. Gu, W. Wang, Z. Cai, F. Xue, Y. Jin and J. Y. Zhu, *Cellulose*, **25**, 2861 (2018).
16. N. Masruchin, B. D. Park, V. Causin and I. C. Um, *Cellulose*, **22**, 1993 (2015).
17. M. Chau, S. E. Sriskandha, D. Pichugin, H. T. Aubin, D. Nykypanchuk, G. Chauve, M. Méthot, J. Bouchard, O. Gang and E. Kumacheva, *Biomacromolecules*, **16**, 2455 (2015).
18. H. Dong, J. F. Snyder, D. T. Tran and J. L. Leadore, *Carbohydr. Polym.*, **95**, 760 (2013).
19. C. Xu, B. Z. Molino, X. Wang, F. Cheng, W. Xu, P. Molino, M. Bacher, D. Su, T. Rosenau, S. Willföra and G. Wallace, *J. Mater. Chem. B.*, **6**, 7066 (2018).
20. W. Xu, X. Wang, N. Sandler, S. Willför and C. Xu, *ACS Sustain. Chem. Eng.*, **6**, 5663 (2018).
21. T. Abitbol, A. Rivkin, Y. Cao, Y. Nevo, E. Abraham, T. B. Shalom, S. Lapido and O. Shoseyov, *Curr. Opin. Biotechnol.*, **39**, 76 (2016).
22. S. Sultan, G. Siqueira, T. Zimmermann and A. P. Mathew, *Curr. Opin. Biomed. Eng.*, **2**, 29 (2017).
23. D. Trache, *AIMS Mater. Sci.*, **5**, 201 (2018).
24. J. M. Dugan, J. E. Gough and S. J. Eichhorn, *Nanomedicine*, **8**, 287 (2013).
25. H. P. S. A. Khalil, A. S. Adnan, E. B. Yahya and N. G. Olaiya, *Polymer*, **12**, 1759 (2020).
26. J. Shojaeiarani, D. Bajwa and A. Shirzadifar, *Carbohydr. Polym.*, **216**, 247 (2019).
27. B. C. Gross, J. L. Erkal, S. Y. Lockwood, C. Chen and D. M. Spence, *Anal. Chem.*, **86**, 3240 (2014).
28. K. Matsumoto, T. Ishiduka, H. Yamada, Y. Yonehara, Y. Arai and K. Honda, *Oral Radiology*, **30**, 98 (2016).
29. J. A. Lewis, *Adv. Funct. Mater.*, **16**, 2193 (2006).
30. Q. Yan, H. Dong, J, Su, J. Han, B. Songa, Q. Wei and Y. Shi, *Engineering*, **4**, 729 (2018).
31. M. Hospodiuk, M. Dey, D. Sosnoski and I. T. Ozbolat, *Biotechnol. Adv.*, **35**, 217 (2017).
32. I. Donderwinkel, J. C. M. Van Hest and N. R. Cameron, *Polym. Chem.*, **8**, 4451 (2017).
33. B. Maiti and D. Díaz, *Polymers*, **10**, 1041 (2018).
34. S. S. Athukoralalage, R. Balu, N. K. Dutta and N. R. Choudhury, *Polymers*, **11**, 1 (2019).
35. S. K. Bhatia and K. W. Ramadurai, *3D printing and bio-based materials in global health*, Springer, Cham (2017).
36. W. Xu, X. Wang, N. Sandler, S. Willför and C. Xu, *ACS Sustain. Chem. Eng.*, **6**, 5663 (2018).
37. C. Xu, B. Z. Molino, X. Wang, F. Cheng, W. Xu, P. Molino, M. Bacher, D. Su, T. Rosenau, S. Willföra and G. Wallace, *J. Mater. Chem. B.*, **6**, 7066 (2018).
38. S. Loai, B. R. Kingston, Z. Wang and D. N. Philpott, *Regen. Med. Front.*, **1**, e190004 (2019).
39. A. Chakrabarty and Y. Teramoto, *Polymers*, **10**, 5 (2018).
40. R. J. Moon, A. Martini, J. Nairn, J. Simonsen and J. Youngblood, *Chem. Soc. Rev.*, **40**, 3941 (2011).
41. J. Cai, J. H. Wu, Z. Lan, J. M. Lin, M. L. Huang, S. C. Hao, T. Sato and S. Yin, *Adv. Mater.*, **19**, 4006 (2007).
42. X. Wen, M. Rajkumar, C. T. Hsu, T. H. Wu, M. G. Chen and C. C. Hu, *Prog. Nat. Sci. Mater. Int.*, **25**, 197 (2015).
43. H. Yu, Z. Qin, B. Liang, N. Liu, Z. Zhou and L. Chen, *J. Mater. Chem. A*, **1**, 3938 (2013).
44. P. Lu and Y. Lo Hsieh, *Carbohydr. Polym.*, **82**, 329 (2010).
45. S. Camarero Espinosa, T. Kuhnt, E. J. Foster and C. Weder, *Biomacromolecules*, **14**, 1223 (2013).
46. H. Sadeghifar, I. Filpponen, S. P. Clarke, D. F. Brougham and D. S. Argyropoulos, *J. Mater. Sci.*, **46**, 7344 (2011).
47. Y. Cao, Y. Jiang, Y. Song, S. Cao, M. Miao, X. Fenga, J. Fang and L. Shi, *Carbohydr. Polym.*, **131**, 152 (2015).
48. H. Kargarzadeh, I. Ahmad, I. Abdullah, A. Dufresne, S. Y. Zainudin and R. M. Sheltami, *Cellulose*, **19**, 855 (2012).
49. X. Lui, Y. Lu and G. Luo, *Ind. Eng. Chem. Res.*, **56**, 8264 (2017).
50. E. E. Ureña-Benavides, G. Ao, V. A. Davis and C. L. Kitchens, *Macromolecules*, **44**, 8990 (2011).
51. R. M. A. Domingues, M. E. Gomes and R. L. Reis, *Biomacromolecules*, **15**, 2327 (2014).
52. M. Cheng, Z. Qin, Y. Chen, J. Liu and Z. Ren, *Cellulose*, **24**, 3243 (2017).
53. Y. Liu, H. Wang, G. Yu, Q. Yu, B. Li and X. Mu, *Carbohydr. Polym.*, **110**, 415 (2014).
54. A. K. Kumar and S. Sharma, *J. Bioresour. Bioprod.*, **4**, 7 (2017).
55. J. Miao, Y. Yu, Z. Jiang and L. Zhang, *Cellulose*, **23**, 1209 (2016).
56. Y. Liu, Y. Liu, B. Guo, Q. Xia, J. Meng, W. Chen, S. Liu, Q. Wang, Y. Liu, J. Li and H. Yu, ACS *Sustain. Chem. Eng.*, **5**, 7623 (2017).
57. A. Khalil, Y. Davoudpour, M. N. Islam, A. Mustapha, K. Sudesh, R. Dungani and M. Jawaidet, *Carbohydr. Polym.*, **99**, 649 (2014).
58. O. Nechyporchuk, M. N. Belgacem and J. Bras, *Ind. Crops Prod.*, **93**, 2 (2016).

59. H. Du, C. Liu, Y. Zhang, G. Yu, C. Si and B. Li, *Ind. Crops Prod.*, **94**, 736 (2016).
60. K. Saelee, N. Yingkamhaeng, T. Nimchua and P. Sukyai, *Ind. Crops Prod.*, **82**, 149 (2016).
61. M. Paako, M. Ankerfors, H. Kosonen, A. Nykänen, S. Ahola, M. Osterberg, J. Ruokolainen, J. Laine, P. T. Larsson, O. Ikkala and T. Lindström, *Biomacromolecules*, **8**, 1934 (2007).
62. T. Saito, Y. Nishiyama, J. L. Putaux, M. Vignon and A. Isogai, *Biomacromolecules*, **7**, 1687 (2006).
63. A. Isogai, T. Saito and H. Fukuzumi, *Nanoscale*, **3**, 71, (2011).
64. W. Im, S. Lee, A. Rajabi Abhari, H. J. Youn and H. L. Lee, *Cellulose*, **25**, 3873 (2018).
65. A. Naderi, T. Lindström and J. Sundström, *Cellulose*, **22**, 1147 (2015).
66. S. Saini, Ç. Yücel Falco, M. N. Belgacem and J. Bras, *Carbohydr. Polym.*, **135**, 239 (2016).
67. T. Saito, I. Shibata, A. Isogai, N. Suguri and N. Sumikawa, *Carbohydr. Polym.*, **61**, 414 (2005).
68. T. Saito and A. Isogai, *Colloids Surf. A*, **289**, 219 (2006).
69. H. Fukuzumi, T. Saito, T. Iwata, Y. Kumamoto and A. Isogai, *Biomacromolecules*, **10**, 162 (2009).
70. A. Chaker and S. Boufi, *Carbohydr. Polym.*, **131**, 224 (2015).
71. U. Islam, M. Ullah and M. W. Khan, *Korean J. Chem. Eng.*, **37**, 925 (2020).
72. P. V. Krasteva, J. B. Bayard, L. Travier, F. A. Martin, P. A. Kaminski, G. Karimova, R. Fronzes and J. M. Ghigo, *Nat. Commun.*, **8**, 25 (2017).
73. J. Trček and F. Barja, *Int. J. Food Microbiol.*, **196**, 137 (2015).
74. J. Škraban, I. Cleenwerck, P. Vandamme, L. Fanedl and J. Trček, *Syst. Appl. Microbiol.*, **41**, 581 (2018).
75. J. Li, G. Chen, R. Zhang, H. Wu, W. Zeng and Z. Liang, *Biotechnol. Appl. Biochem.*, **66**, 108 (2019).
76. C. Castro, M. Castro, M. Osorio, M. T. Taborda, B. Gómez, R. Zuluaga, C. Gómez, P. Gañán, O. J. Rojas and C. Castro, *Int. J. Syst. Evol. Microbiol.*, **63**, 1119 (2013).
77. J. L. W. Morgan, J. Strumillo and J. Zimmer, *Nature*, **493**, 181 (2013).
78. P. Ross, R. Mayer and M. Benziman, *Microbiol. Rev.*, **55**, 35 (1991).
79. J. T. McNamara, J. L. W. Morgan and J. Zimmer, *Annu. Rev. Biochem.*, **84**, 895 (2015).
80. M. V. Zugravu, R. A. Smith, B. T. Reves, J. A. Jennings, J. O. Cooper, W. O. Haggard and J. D. Bumgardner, *J. Biomater. Appl.*, **28**, 566 (2013).
81. O. Wichterle and D. Lim, *Nature*, **185**, 117 (1960).
82. D. A. Gyles, L. D. Castro, J. O. C. Silva and R. M. Ribeiro-Costa, *Eur. Polym. J.*, **88**, 373 (2017).
83. M. Chau, K. J. France, B. Kopera, V. R. Machado, S. Rosenfeldt, L. Reyes, J. W. Chan, S. Förster, E. D. Cranston, T. Hoare and E. Kumacheva, *Chem. Mater.*, **28**, 3406 (2016).
84. D. M. Nascimento, D. M. Nascimento, Y. L. Nunes, M. C. Figueirêdo, H. M. Azeredo, F. A. Aouada, P. A. Feitosa, M. F. Rosa and A. Dufresne, *Green Chem.*, **20**, 2428 (2018).
85. K. J. De France, T. Hoare and E. D. Cranston, *Chem. Mater.*, **29**, 4609 (2017).
86. J. W. McAllister, P. W. Schmidt, K. D. Dorfman, T. P. Lodge and F. S. Bates, *Macromolecules*, **48**, 7205 (2015).
87. H. Kargarzadeh, J. Huang, N. Lin, I. Ahmad, M. Marianoe, A. Dufresnee, S. Thomas and A. Gałęskia, *Prog. Polym. Sci.*, **87**, 197 (2018).
88. K. Oksman, Y. Aitomäki, A. P. Mathewa, G. Siqueirac, Q. Zhou, S. Butylina, S. Tanpichai, X. Zhoua and S. Hooshmanda, *Compos. Part A Appl. Sci. Manuf.*, **83**, 2 (2016).
89. S. Deng, S. Binauld, G Mangiante, J. M. Frances and A. Charlot, *Carbohydr. Polym.*, **151**, 899 (2016).
90. Z. Zhang, G. Sèbe, D. Rentsch, T. Zimmermann and P. Tingaut, *Chem. Mater.*, **26**, 2659 (2014).
91. J. Sethi, M. Farooq, S. Sain, M. Sain, J. A. Sirviö, M. Illikainen and K. Oksman, *Cellulose*, **25**, 259 (2018).
92. Q. Wang, H. Du, F. Zhang, Y. Zhang, M. Wu, G. Yu, C. Liu, B. Li and H. Penga, *J. Mater. Chem. A*, **6**, 13021 (2018).
93. J. S. Gonzalez, L. N. Ludueña, A. Ponce and V. A. Alvarez, *Mater. Sci. Eng. C*, **34**, 54 (2014).
94. J. Han, T. Lei and Q. Wu, *Cellulose*, **20**, 2947 (2013).
95. S. K. Bajpai, V. Pathak, B. Soni and Y. M. Mohan, *Carbohydr. Polym.*, **106**, 351 (2014).
96. Y. Chen, W. Xu, W. Liu and G. Zeng, *J. Mater. Res.*, **30**, 1797 (2015).
97. N. Lin and A. Dufresne, *Biomacromolecules*, **14**, 871 (2013).
98. C. Spagnol, H. A. Francisco, G. B. Pereira, A. R. Fajardoa, A. F. Rubira and E. C. Muniz, *Carbohydr. Polym.*, **87**, 2038 (2012).
99. S. Y. Ooi, I. Ahmad and M. C. I. M. Amin, *Ind. Crops Prod.*, **93**, 227 (2016).
100. N. Lin, A. Gè, D. Wouessidjewe, J. Huang and A. Dufresne, *ACS Appl. Mater. Interfaces*, **8**, 6880 (2016).
101. K. Wang, K. C. Nune and R. D. K. Misra, *Acta Biomater.*, **36**, 143 (2016).
102. J. You, J. Cao, Y. Zhao, L. Zhang, J. Zhou and Y. Chen, *Biomacromolecules*, **17**, 2939 (2016).
103. T. S. Anirudhan and S. R. Rejeena, *J. Appl. Polym. Sci.*, **131**, 8657 (2014).
104. M. R. Mauricio, P. G. Da Costa, S. K. Haraguchi, M. R. Guilherme, E. C. Muniz and A. F. Rubira, *Carbohydr. Polym.*, **115**, 715 (2015).
105. R. M. Domingues, M. Silva, P. Gershovich, S. Betta, P. Babo, S. G. Caridade, J. F. Mano, A. Motta, R. L. Reis and M. E. Gomes, *Bioconjugate Chem.*, **26**, 1571 (2015).
106. W. Li, Y. Lan, R. Guo, Y. Zhang, W. Xue and Y. Zhang, *J. Biomater. Appl.*, **29**, 882 (2015).
107. A. B. Fall, S. B. Lindström, J. Sprakel Cd and L. Wågberg, *Soft Matter*, **9**, 1852 (2013).
108. P. Laurén, Y. R. Lou, M. Raki, A. Urtti, K. Bergström and M. Yliperttula, *Eur. J. Pharm. Sci.*, **65**, 79 (2014).
109. N. Masruchin, B. D. Park, V. Causin and I. C. Um, *Cellulose*, **22**, 1993 (2015).
110. G. T. Rendon, T. Femmer, L. D. Laporte, T. Tigges, K. Rahimi, F. Gremse, S. Zafarnia, W. Lederle, S. Ifuku, M. Wessling, J. G. Hardy and A. Walther, *Adv. Mater.*, **27**, 2989 (2015).
111. S. Spoljaric, A. Salminen, N. D. Luong and J. Seppälä, *Eur. Polym. J.*, **56**, 105 (2014).
112. C. Eyholzer, A. B. Couraça, F. Duc, P. E. Bourban, P. Tingaut, T. Zimmermann, J. A. E. Månson and K. Oksman, *Biomacromolecules*, **12**, 1419 (2011).
113. N. Naseri, J. M. Poirier, L. Girandon, M. Fröhlich, K. Oksman and A. P. Mathew, *RSC Adv.*, **6**, 5999 (2016).
114. J. Liu, G. C. Carrasco, F. Cheng, W. Xu, S. Willför, K. Syverud and C. Xu, *Cellulose*, **23**, 3129 (2016).

115. I. Sulaeva, H. Hettegger, A. Bergen, C. Rohrer, M. Kostic, J. Konnerth, T. Rosenau and A. Potthast, *Mater. Sci. Eng. C*, **110**, 110619 (2020).
116. M. Pandey, N. Mohamad, W. L. Low, C. Martin and M. C. I. Mohd Amin, *Drug Deliv. Transl. Res.*, **7**, 89 (2017).
117. A. E. Way, L. Hsu, K. Shanmuganathan, C. Weder and S. J. Rowan, *ACS Macro Lett.*, **1**, 1001 (2012).
118. N. Lin and A. Dufresne, *Biomacromolecules*, **14**, 871 (2013).
119. J. R. McKee, E. A. Appel, J. Seitsonen, E. Kontturi, O. A. Scherman and O. Ikkala, *Adv. Funct. Mater.*, **24**, 2706 (2014).
120. T. Abitbol, T. Johnstone, T. M. Quinn and D. G. Gray, *Soft Matter*, **7**, 2373 (2011).
121. J. S. Gonzalez, L. N. Ludueña, A. Ponce and V. A. Alvarez, *Mater. Sci. Eng. C*, **34**, 54 (2014).
122. C. Spagnol, F. Rodrigues, A. G. Neto, G. B. Pereira, A. R. Fajardo, E. Radovanovic, A. F. Rubira and E. C. Muniz, *Eur. Polym. J.*, **48**, 454 (2012).
123. J. Yang, C. R. Han, X. M. Zhang, F. Xu and R. C. Sun, *Macromolecules*, **47**, 4077 (2014).
124. J. Yang, C. R. Han, F. Xu and R. C. Sun, *Nanoscale*, **6**, 5934 (2014).
125. J. Yang, X. M. Zhang and F. Xu, *Macromolecules*, **48**, 1231 (2015).
126. N. B. Palaganas, J. D. Mangadlao, A. Christopher, J. O. Palaganas, K. D. Pangilinan, Y. J. Lee and R. C. Advincula, *ACS Appl. Mater. Interfaces*, **9**, 34314 (2017).
127. J. Wang, A. Chiappone, I. Roppolo, F. Shao, E. Fantino, M. Lorusso, D. Rentsch, K. Dietliker, C. F. Pirri and H. Grützmacher, *Angew. Chem. - Int. Ed.*, **57**, 2353 (2018).
128. J. Yang, J. J. Zhao, C. R. Han, J. F. Duan, F. Xu and R. C. Sun, *Cellulose*, **21**, 541 (2014).
129. S. Sultan and A. P. Mathew, *Nanoscale*, **10**, 4421 (2018).
130. A. Kumar, I. A. I. Matari and S. S. Han, *Biofabrication*, **12**, 025029 (2020).
131. H. Dong, J. F. Snyder, K. S. Williams and J. W. Andzelm, *Biomacromolecules*, **14**, 3338 (2013).
132. N. E. Zander, H. Dong, J. Steele and J. T. Grant, *ACS Appl. Mater. Interfaces*, **6**, 618502 (2014).
133. J. Yang and F. Xu, *Biomacromolecules*, **18**, 2623 (2017).
134. W. Kong, C. Wang, C. Jia, Y. Kuang, G. Pastel, C. Chen, G. Chen, S. He, H. Huang, J. Zhang, S. Wang and L. Hu, *Adv. Mater.*, **30**, 1, (2018).
135. J. G. Torres-Rendon, T. Femmer, L. D. Laporte, T. Tigges, K. Rahimi, F. Gremse, S. Zafarnia and W. Lederle, *Adv. Mater.*, **27**, 2989 (2015).
136. S. Shin, S. Park, M. Park, E. Jeong, K. Na, H. J. Youn and J. Hyun, *BioResources*, **12**, 2941 (2017).
137. R. D. Chen, C. F. Huang and S. Hsu, *Carbohydr. Polym.*, **212**, 75 (2019).
138. J. G. Torres-Rendon, T. Femmer, L. D. Laporte, T. Tigges, K. Rahimi, F. Gremse, S. Zafarnia and W. Lederle, *Adv. Mater.*, **27**, 2989 (2015).
139. P. Cerrutti, P. Roldán, R. M. García, M. A. Galvagno, A. Vázquez and M. L. Foresti, *J. Appl. Polym. Sci.*, **133**, 1 (2016).
140. Z. Hussain, W. Sajjad, T. Khan and F. Wahid, *Cellulose*, **26**, 2895 (2019).
141. M. Moniri, A. B. Moghaddam, S. Azizi, A. Rahim, A. B. Ariff, W. Z. Saad, M. Navaderi and R. Mohamad, *Nanomaterials*, **7**, 1 (2017).
142. N. Shah, M. Ul-Islam, W. A. Khattak and J. K. Park, *Carbohydr. Polym.*, **98**, 1585 (2013).
143. W. Ye, X. Li, H. Zhu, X. Wang, S. Wang, H. Wang and R. Sun, *Chem. Eng. J.*, **299**, 45 (2016).
144. S. Perumal, R. Atchudan, D. H. Yoon and I. W. Cheong, *J. Mater. Sci.*, **55**, 9354 (2020).
145. S. Perumal, R. Atchudan and I. W. Cheong, *Int. J. Hydrogen Energy*, **46**, 10850 (2021).
146. S. Perumal, H. M. Lee and I. W. Cheong, *J. Adhes. Interface*, **20**, 53 (2019).
147. H. Luo, J. Dong, X. Xu, J. Wang, Z. Yang and Y. Wan, *Compos. Part A Appl. Sci. Manuf.*, **109**, 290 (2018).
148. B. Luppi, F. Bigucci, T. Cerchiara and V. Zecchi, *Expert Opin. Drug Deliv.*, **7**, 811 (2010).
149. R. Li, P. Hu, X. Ren, S. D. Worley and T. S. Huang, *Carbohydr. Polym.*, **92**, 534 (2013).
150. R. C. Chien, M. T. Yen and J. L. Mau, *Carbohydr. Polym.*, **138**, 259 (2016).
151. N. R. Sudarshan, D. G. Hoover and D. Knorr, *Food Biotechnol.*, **6**, 257 (1992).
152. M. S. Toivonen, S. Kurki-Suonio, F. H. Schacher, S. Hietala, O. J. Rojas and O. Ikkala, *Biomacromolecules*, **16**, 1062 (2015).
153. I. Cielecka, M. Szustak, H. Kalinowska, E. G. Darmach, M. Ryngajłło, W. Maniukiewicz and S. Bielecki, *Cellulose*, **26**, 5409 (2019).
154. F. Wahid, X. H. Hu, L. Q. Chu, S. R. Jia, Y. Y. Xie and C. Zhong, *Int. J. Biol. Macromol.*, **122**, 380 (2019).
155. Q. Wang, T. A. Asoh and H. Uyama, *RSC Adv.*, **8**, 12608 (2018).
156. N. Yuan, L. Xua, L. Zhanga, H. Ye, J. Zhaoa, Z. Liu and J. Ronga, *Mater. Sci. Eng. C.*, **67**, 221 (2016).
157. P. J. O'Brien, A. G. Siraki and N. Shangari, *Crit. Rev. Toxicol.*, **35**, 609 (2005).
158. J. P. Kehrer and S. S. Biswal, *Toxicol. Sci.*, **576**, 15 (2000).
159. S. Mulijani, Erizal, T. T. Irawadi and T. C. Katresna, *Adv. Mater. Res.*, **974**, 91 (2014).
160. N. Mohamad, F. Buang, A. Mat Lazim, N. Ahmad, C. Martin and M. C. I. Mohd Amin, *J. Biomed. Mater. Res. Part B Appl. Biomater.*, **105**, 2553 (2017).
161. P. Apelgren, E. Karabulut, M. Amoroso, A. Mantas, H. M. Ávila, L. Kölby, T. Kondo, G. Toriz and P. Gatenholm, *ACS Biomater. Sci. Eng.*, **5**, 2482 (2019).
162. E. Caló and V. V. Khutoryanskiy, *Eur. Polym. J.*, **65**, 252 (2015).
163. M. S. Chapekar, *J. Biomed. Mater. Res.*, **53**, 617 (2002).
164. L. Y. Zhu, X. Q. Yan and H. M. Zhang, *Korean J. Chem. Eng.*, **32**, 369 (2015).
165. F. M. Chen and X. Liu, *Prog. Polym. Sci.*, **53**, 86 (2016).
166. M. Fiayaz, K. M. Zia and M. A. Javaid, *Korean J. Chem. Eng.*, **37**, 2351 (2020).
167. E. Y. Loh, M. B. Fauzi, M. H. Ng, P. Yuen, S. Fern, H. Ariffin, M. C. Iqbal and M. Amin, *ACS Appl. Mater. Interfaces*, **10**, 39532 (2018).
168. M. Osorio, O. P. Gañána, T. Naranjob, R. Zuluagaa, T. G. Kootend and C. Castroa, *Mater. Sci. Eng. C.*, **100**, 697 (2019).
169. M. Roman, A. P. Haring and T. J. Bertucio, *Curr. Opin. Chem. Eng.*, **24**, 98 (2019).
170. N. Halib, I. Ahmad, M. Grassi and G. Grassi, *Int. J. Pharm.*, **566**,

631 (2019).
171. D. Ficai, M. G. Albu, M. Sonmez, A. Ficai and E. Andronescu, *Nanobiomater. Soft Tissue Eng.*, **5**, 355 (2016).
172. C. Republic, *Physiol. Res.*, **67**, S335 (2018).
173. B. Pei, W. Wang, Y. Fan, X. Wang, F. Watari and X. Li, *Regen. Biomater.*, **4**, 257 (2017).
174. F. J. O'Brien, *Mater. Today*, **14**, 88 (2011).
175. R. Hobzova, J. Hrib, J. Sirc, E. Karpushkin, J. Michalek, O. Janouskova and P. Gatenholm, *J. Nanomater.*, **2018**, 5217095 (2018).
176. L. Lamboni, C. Xu, J. Clasohm, J. Yang, M. Saumer, K. H. Schäfer and G. Yanga, *Mater. Sci. Eng. C.*, **102**, 502 (2019).
177. L. Huang, *Carbohydr. Polym.*, **221**, 146 (2019).
178. M. Liu, X. Zeng, C. Ma, H. Yi, Z. Ali, X. Mou, S. Li, Y. Deng and N. He, *Bone Res.*, **5**, 17014 (2017).
179. C. Huang, N. Hao, S. Bhagiac, M. Li, X. Meng, Y. Pue, Q. Yonga and A. J. Ragauskascde, *Materialia*, **4**, 237 (2018).
180. X. Yang, E. Bakaic, T. Hoare and E. D. Cranston, *Biomacromolecules*, **14**, 4447 (2013).
181. L. Dai, T. Cheng, C. Duan, W. Zhao, W. Zhang, X. Zou, J. Aspler and Y. Ni, *Carbohydr. Polym.*, **203**, 71 (2019).
182. C. C. Piras, S. Fernández-Prieto and W. M. De Borggraeve, *Biomater. Sci.*, **5**, 1988 (2017).
183. Q. Wang, J. Sun, Q. Yao, C. Ji, J. Liu and Q. Zhu, *Cellulose*, **25**, 4275 (2018).
184. T. S. Jang, H. D. Jung, H. M. Pan, W. T. Han, S. Chen and J. Song, *Int. J. Bioprinting*, **4**, 1 (2018).
185. J. Wei, B. Wang, Z. Li, Z. Wu, M. Zhang, N. Sheng, Q. Liang, H. Wang and S. Chen, *Carbohydr. Polym.*, **238**, 116207 (2020).
186. K. Markstedt, A. Mantas, I. Tournier, H. Martínez Ávila, D. Hägg and P. Gatenholm, *Biomacromolecules*, **16**, 1489 (2015).
187. H. Martínez Ávila, S. Schwarz, N. Rotter and P. Gatenholm, *Bioprinting*, **1**, 22 (2016).
188. R. E. Abouzeid, R. Khiari, D. Beneventi and A. Dufresne, *Biomacromolecules*, **19**, 4442 (2018).
189. E. A. Kamoun, E. R. S. Kenawy and X. Chen, *J. Adv. Res.*, **8**, 217 (2017).
190. H. Hamedi, S. Moradi, S. M. Hudson and A. E. Tonelli, *Carbohydr. Polym.*, **199**, 445 (2018).
191. J. Liu, G. C. Carrasco, F. Cheng, W. Xu, S. Willför, K. Syverud and C. Xu, *Cellulose*, **23**, 3129 (2016).
192. W. Huang, Y. Wang, Z. Huang, X. Wang, L. Chen, Y. Zhang and L. Zhang, *ACS Appl. Mater. Interfaces*, **10**, 41076 (2018).
193. A. Khalid, R. Khan, M. Ul-Islam, T. Khan and F. Wahid, *Carbohydr. Polym.*, **164**, 214 (2017).
194. A. Khalid, H. Ullah, M. U. Islam, R. Khan, S. Khan, F. Ahmad, T. Khan and F. Wahid, *RSC Adv.*, **7**, 47662 (2017).
195. R. Liu, L. Dai, C. Si and Z. Zeng, *Carbohydr. Polym.*, **195**, 63 (2018).
196. H. M. Manukumar, S. Umesha and H. N. N. Kumar, *Int. J. Biol. Macromol.*, **102**, 1257 (2017).
197. A. Basu, J. Lindh, E. Ålander, M. Strømme and N. Ferraz, *Carbohydr. Polym.*, **174**, 299 (2017).
198. A. Basu, K. Heitz, M. Strømme, K. Welch and N. Ferraz, *Carbohydr. Polym.*, **181**, 345 (2018).
199. Y. Liu, Y. Sui, C. Liu, C. Liu, M. Wu, B. Li and Y. Li, *Carbohydr. Polym.*, **188**, 27 (2018).
200. M. Khamrai, S. L. Banerjee, S. Paul, A. K. Ghosh, P. Sarkar and P. P. Kundu, *ACS Sustain. Chem. Eng.*, **7**, 12083 (2019).
201. S. Jiji, S. Udhayakumar, C. Rose, C. Muralidharan and K. Kadirvelu, *Int. J. Biol. Macromol.*, **122**, 452 (2019).
202. H. Dong, L. Zheng, P. Yu, Q. Jiang, Y. Wu, C. Huang and B. Yin, *ACS Sustain. Chem. Eng.*, **8**, 256 (2020).
203. H. Adlercreutz, *Environ. Health Perspect.*, **7**, 103 (1995).
204. J. L. Espinoza-Acosta, P. I. Torres-Chávez, B. Ramírez-Wong, C. M. López-Saiz and B. Montaño-Leyva, *BioResources*, **11**, 5452 (2016).
205. P. R. F. de S. Moraes, S. Saska, H. Barud, L. R. de Lima, V. da C. A. Martins, A. M. de G. Plepis, S. J. L. Ribeiro and A. M. M. Gaspar, *Mater. Res.*, **19**, 106 (2016).
206. S. R. Van Tomme and W. E. Hennink, *Expert Rev. Med. Devices*, **4**, 147 (2007).
207. N. Mohamad, M. C. I. Mohd Amin, M. Pandey, N. Ahmad and N. F. Rajab, *Carbohydr. Polym.*, **114**, 312 (2014).
208. M. Pandey, N. Mohamad and W. L. Low, *Drug Deliv. Transl. Res.*, **7**, 89 (2017).
209. P. Gupta, K. Vermani and S. Garg, *Drug Discov. Today*, **7**, 569 (2002).
210. C. Chuah, J. Wang, J. Tavakoli and Y. Tang, *Polymers*, **10**, 1323 (2018).
211. N. Mohamad, E. Y. X. Loh, M. B. Fauzi, M. H. Ng and M. C. I. Mohd Amin, *Drug Deliv. Transl. Res.*, **9**, 444 (2019).
212. E. Y. X. Loh, N. Mohamad, M. B. Fauzi, M. H. Ng, S. F. Ng and M. C. I. Mohd Amin, *Sci. Rep.*, **8**, 1 (2018).
213. D. Plackett, K. Letchford, J. Jackson and H. Burt, *Nord. Pulp Pap. Res. J.*, **29**, 105 (2014).
214. Y. Xue, Z. Mou and H. Xiao, *Nanoscale*, **9**, 14758 (2017).
215. C. A. García-González, M. Alnaief and I. Smirnova, *Carbohydr. Polym.*, **86**, 1425 (2011).
216. W. Li, Y. Lan, R. Guo, Y. Zhang, W. Xue and Y. Zhang, *J. Biomater. Appl.*, **29**, 882 (2015).
217. N. Lin, A. Gèze, D. Wouessidjewe, J. Huang and A. Dufresne, *ACS Appl. Mater. Interfaces*, **8**, 6880 (2016).
218. J. Supramaniam, R. Adnan, N. H. Mohd Kaus and R. Bushra, *Int. J. Biol. Macromol.*, **118**, 640 (2018).
219. M. Åhlén, G. K. Tummala and A. Mihranyan, *Int. J. Pharm.*, **536**, 73 (2018).
220. P. Laurén, Y. R. Lou, M. Raki, A. Urtti, K. Bergström and M. Yliperttula, *Eur. J. Pharm. Sci.*, **65**, 79 (2014).
221. H. Paukkonen, M. Kunnari, P. Laurén, T. Hakkarainen, V. V. Auvinen, T. Oksanen, R. Koivuniemi, M. Yliperttula and T. Laaksonen, *Int. J. Pharm.*, **532**, 269 (2017).
222. H. Zhang, *ACS Sustain. Chem. Eng.*, **4**, 13924 (2018).
223. T. Paulraj, A. V. Riazanova and A. J. Svagan, *Acta Biomater.*, **69**, 196 (2018).
224. D. Psimadas, P. Georgoulias, V. Valotassiou and G. Loudos, *J. Pharm. Sci.*, **101**, 2271 (2012).
225. M. Badshah, H. Ullah, A. R. Khan, S. Khan, J. K. Park and T. Khan, *Int. J. Biol. Macromol.*, **113**, 526 (2018).
226. H. Luo, H. Ao, G. Li, W. Lia, G. Xiong, Y. Zhu and Y. Wanab, *Curr. Appl. Phys.*, **17**, 249 (2017).
227. W. Treesuppharat, P. Rojanapanthu, C. Siangsanoh, H. Manuspiya and S. Ummartyotin, *Biotechnol. Reports*, **15**, 84 (2017).

228. J. Wei, B. Wang, Z. Li, Z. Wu, M. Zhang, N. Sheng, Q. Liang, H. Wang and S. Chen, *Carbohydr. Polym.*, **238**, 116207 (2020).
229. T. Hakkarainen, R. Koivuniemi, M. Kosonen, C. E. Lucea, A. S. Garcia, J. Vuola, J. Valtonen, P. Tammela, A. Mäkitie, K. Luukko, M. Yliperttula and H. Kavola, *J. Contr. Release*, **244**, 292 (2016).
230. A. B. Seabra, J. S. Bernardes, W. J. Fávaro, A. J. Paula and N. Durán, *Carbohydr. Polym.*, **181**, 514 (2018).
231. R. Koivuniemi, T. Hakkarainen, J. Kiiskinen, M. Kosonen, J. Vuola, J. Valtonen, K. Luukko, H. Kavola and M. Yliperttula, *Adv. Wound Care*, **9**, 199 (2019).
232. P. Apelgren, M. Amoroso, A. Lindahl, C. Brantsing, N. Rotter, P. Gatenholm and L. Kölby, *PLoS ONE*, **12**, 12 (2017).

In Woo Cheong obtained B.S., M.S., and Ph.D degree in Chem. Eng. at Yonsei Univ., Korea, in 1995, 1997, and 2001, respectively. From 2002 to 2004, he was a postdoctoral fellow at Sydney University and Yonsei University. He joined Kyungpook National University (KNU) in 2005 and is currently a professor in Dept. Appl. Chem. in KNU. He published more than 150 papers and 30 international and domestic patents. He is also the Chief Editor of J. Adhes. Interface (2020. 1.~ present) and has been recognized with several awards including Best Lecture Awards (KNU, 2008, 2010), Excellent Researcher (KNU, JCR 5% - 2018, 2021), and Best Lecture Award (KSEE, 2020).